RSC Applied Polymers

ROYAL SOCIETY OF CHEMISTRY

REVIEW

View Article Online
View Journal | View Issue

Cite this: *RSC Appl. Polym.*, 2024, **2**, 775

Polyaniline (PANI) nanocomposites with Se, Te and their metal chalcogenides: a review

Alok Kumar Yadav,[a] Naeem Mohammad,[a] Elham Chamanehpour,[b] Yogendra Kumar Mishra [b] and Pawan K. Khanna *[a]

Research over the past four decades on polyaniline has matured, and consequently it has become one of the most popular conducting polymers. Also, several methods have been proposed by researchers for the synthesis and conversion of polyaniline (PANI) to various forms as well as its doping with chalcogens especially selenium (Se) and tellurium (Te). These composites have been explored using various chemical methods and their different properties have been extensively studied in terms of electrical, thermal, morphological and optical behaviour. This review summarizes the results from research experiments, including their synthesis and characterization, and the study of their various properties such as DC conductivity measurements, scanning electron microscopy (SEM), Fourier transform infrared (FTIR) spectroscopy, field emission studies, EMI shielding behaviour, and electrochemical, supercapacitive, optoelectronic and thermoelectric properties. The incorporation of chalcogens in PANI leads to a significant improvement in its electrical conductivity and field emission properties, making the resulting nanocomposites promising materials for various electronic applications. The global energy crisis underscores the need for innovative materials for the production of energy. In this case, solution-based polymer thermoelectric (TE) technologies offer an eco-friendly and cost-effective approach to convert heat into electricity. The successful electrodeposition of tellurium films onto phenolic foam with PANI coatings and the synthesis of novel PANI/Te nanocomposites with enhanced nonlinear optical properties open up new avenues. These nanocomposites were prepared using different methods including simultaneous electrochemical reactions, *in situ* polymerization, and interfacial polymerization.

Received 13th March 2024,
Accepted 26th June 2024

DOI: 10.1039/d4lp00093e

rsc.li/rscapplpolym

1. Introduction

Advanced materials such metals and ceramics including polymer composites are versatile materials and are the basis for modern technological advancement. The advent of conducting polymers (CPs) was a significant finding by researchers, where it was demonstrated that the conductivity of polyacetylene can be increased by adding electron acceptors, with the Nobel prize awarded in 2000 to Shirakawa, Heeger, and MacDiarmid for this achievement.[1,2] One of the well-known and extensively researched conducting polymers is polyaniline (PANI). Additionally, PANI has been doped with a range of chemicals including protonic acids and oxidants, and it can be tailored for ease of processing into various forms such as coatings. PANI has been demonstrated to be useful for a range of applications including batteries,[3] supercapacitors[4] and sensors.[5] It is environmentally sustainable and stable, relatively inexpensive, simple to synthesize, and has a high charge storage density. The oxidation and protonation states of polyaniline govern its physical and electrochemical properties.[6] PANI has been considered a desirable conductive material since its discovery to synthesize conductive composites for a variety of uses, including electro-magnetic (EM) absorption, particularly microwave absorption, dissipation of electricity, heating probes, conducting glues, conducting membranes, anticorrosion paint/coatings, and sensor materials.[5,7–9] However, although PANI has a variety of uses in large-scale industrial applications, many of its prospective uses have not been fully investigated to date due to its difficult processing. Therefore, the development of preparation strategies and accurate molecular design are desirable to facilitate the synthesis of primary conducting polymers. Typically, the polymerization of aniline leads to the formation of polyaniline, which has a conjugated structure with a rigid backbone, *i.e.* alternating single–double bonds. Researchers

[a]*Quantum Dots/Nanomaterials Laboratory, Department of Applied Chemistry, Defence Institute of Advanced Technology, Pune 411025, India.*
E-mail: pawankhanna2002@yahoo.co.in, khannap@diat.ac.in
[b]*University of Southern Denmark, Alsion 2, 6400 Sønderborg, Denmark*

have proposed that PANI can exist in several oxidation states, as follows:[8,10]

1. Leucoemeraldine – a fully reduced form of polyaniline,

2. Pernigraniline – reported to be a fully oxidized form of polyaniline and

3. Emeraldine salt/base – green/blue as oxidized : reduced (1 : 1).

Amongst them, emeraldine is the most conductive form of PANI. The conductivity of emeraldine base (EB) is lower than that of emeraldine salt (ES) because EB exhibits semiconducting nature, whereas ES possesses metallic conductivity. When the emeraldine base undergoes protonation to become the emeraldine salt, a structural transformation occurs due to the mechanism of proton-induced spin unpairing. Consequently, this leads to a band that is half-filled, potentially giving rise to a metallic state, where each repeating unit carries a positive charge due to protonation, together with an associated counter ion. The conductivity is also affected by the synthesis processes and parameters involved. The conductivity of EB has been reported to increase with acid doping.[8] Aqueous solutions of acids such as camphor sulfonic acid (CSA), picric acid, phosphoric acid, sulfuric acid, and hydrochloric acid were used for doping EB PANI. However, its limited dissolution behaviour hinders its practical applications. The difficult processibility of PANI is attributed to the possible hydrogen bonding between the atoms of its adjacent chains and its stiff polymer backbone. Also, the melt processing of PANI is excluded because of the instability of its EB form at melt-processing temperatures.[8,10] However, due to its distinctive oxidation states, the doping mechanism in polyaniline stands out among conducting polymers. Considering the aforementioned discoveries, the core idea of polyaniline synthesis, doping, and conduction mechanism offers in-depth research for both additional technological applications and fundamental scientific interest.[8–11] Several metals have been incorporated in polyaniline to study its properties, including Ag/PANI,[12] Au/PANI,[13] Zn/PANI,[3] and Pt/PANI.[14] Sezer *et al.*[12] measured the intensity-dependent refractive index of a PANI/Ag nanocomposite and found that it is suitable for optical pulse compression and limiting due to its reversible absorption behaviour at the same wavelength. Li *et al.*[13] constructed AuNP@PANI nanospheres by oxidizing aniline using $HAuCl_4$ oxidant with the simultaneous formation of Au NPs. Li *et al.*[3] incorporated Zn microspheres in self-assembled hollow microspheres of PANI to form a PANI hollow microsphere/zinc composite. Zhang *et al.*[14] deposited a PANI array on carbon cloth by chronoamperometry (applying a time-dependent square wave potential to working electrode), and then on a Pt nanosheet by amperometry (applying a constant potential to the working electrode) to detect ammonia. Likewise, several metal oxides have also been introduced in the polyaniline network to generate a variety of conducting polymer nano-composites. For example, ZnO/PANI,[15] CdO/PANI,[16] CuO/PANI,[17] and TiO_2/PANI.[18] Gheymasi *et al.*[15] copolymerized aniline and pyrrole using ammonium peroxydisulphate (APS) as an oxidant and T-X100 as an emulsifier, and then blended it with ZnO nanoparticles in $CHCl_3$ solution to obtain self-focusing and reverse saturation absorption, which led to its use for the protection of the eyes and optical instruments from high-intensity lasers. Roy *et al.*[16] reported the preparation of a CdO/PANI composite *via* an *in situ* polymerization process using aniline–HCl–CdO solution and APS. Due to the structural changes upon the introduction of CdO, the conductivity increased. In the small frequency region, the AC conductivity deviated from Jonscher's power law based on the dipole polarization effect, $\sigma(\omega) = \sigma_o + A\omega^n$.

Alok Kumar Yadav

Alok Kumar Yadav obtained his BSc from Dr Ram Manohar Lohia Avadh University, Ayodhya, Uttar Pradesh, India in 2018. He completed his MSc Degree in Physics in 2021 from the Central University of Jharkhand, India. In 2023, he obtained his MTech in Nano Science and Technology under the supervision of Prof. Pawan Kumar Khanna from the Defence Institute of Advanced Technology (DIAT), Pune, India. Presently, he is pursuing his PhD in Materials Science at the Indian Institute of Technology (IIT), Kanpur, India. Research interests: nanomaterial, nanocomposites and their EMI shielding application.

Naeem Mohammad

Naeem Mohammad obtained his BSc and MSc degrees from the University of Kota, Kota, Rajasthan, India in 2018 and 2020, respectively. During his undergrad and postgrad studies, he received a scholarship for higher education (SHE) under the INSPIRE Scheme "Innovation in Science Pursuit for Inspired Research (INSPIRE)" from the Department of Science & Technology (DST), Govt. of India. In 2022, he was selected for a doctoral fellowship under the INSPIRE scheme from DST, and presently he is working as an INSPIRE Fellow and pursuing his PhD under the guidance of Prof. P. K. Khanna at the Defence Institute of Advanced Technology, Pune, India. His research interests include metal chalcogenides, nanomaterials, quantum dots, materials chemistry and their EMI shielding, photocatalysis, and thermoelectric applications.

Thampi *et al.*[17] grew brown-coloured 50 nm CuO NPs using copper nitrate and polyethylene glycol and immobilized them in a PANI matrix *via* the *in situ* polymerization of aniline. The as-generated composite was incorporated in woven and non-woven cotton fabric by immersing it in PANI/CuO solution for anti-bacterial applications. Gapusan *et al.*[18] immobilized TiO_2 NPs in PANI-coated kapok fibres *via* the hydrothermal method, which demonstrated photocatalytic activity against methyl orange (MO) and Cr(IV) and antibacterial activity against *E. coli* under visible light. Similarly, a variety of other oxide nanoparticles, such as TiO_2, CeO_2, ZrO_2, Fe_2O_3, Fe_3O_4, ZnO, and CdO could be incorporated in a polymer matrix and are useful for a variety of applications in various scientific and technological fields (Scheme 1).[10,16–18]

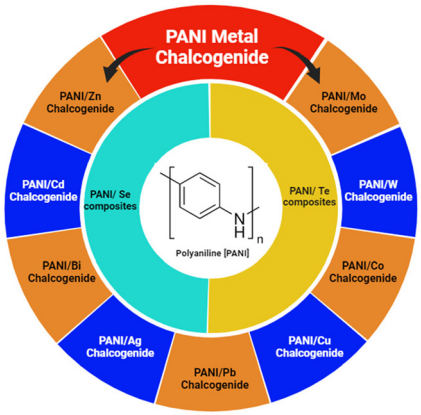

Scheme 1 Bird's eye view of various PANI/chalcogen composites.

2. PANI-chalcogen (Se & Te) nanocomposites

Chalcogens are elements of group 16 (O, S, Se, Te and Po). However, oxygen and polonium are not considered true chalcogens. In the case of oxygen (O_2), this mainly due to its difference in chemical properties owing to the absence of vacant d-orbitals. Alternatively, in the heavier chalcogens, they possess vacant d-orbitals, and thus show diverse chemical and physical properties. Also, the electronegativity (EN) of oxygen is much higher than that of the other chalcogens. Polonium is a heavier element as well as radioactive element. The chemical properties of selenium and tellurium have opened up new avenues in the field of electrical and opto-electronic applications, and therefore inorganic metal chalcogenides have attracted immense attention from researchers globally. Recently, Se and Te-based nanocomposites have had a huge impact due to their superior electrical, thermal and optical properties. This has also been extended to their nanocomposites with conducting polymers, *e.g.* PANI, for further advancement. Amongst the conducting polymers, polyaniline has not been widely studied with Se and Te, although their combination as a nanocomposite can result in significant changes in their properties. Thus, the scope of this review is limited to investigating the effects of the incorporation of selenium (Se), tellurium (Te) and their inorganic selenides and tellurides on the properties of PANI. Some research has been conducted on these materials to discover their applications in supercapacitors, thermoelectric, electrical, opto-electronic, medicinal and other fields (Table 1).

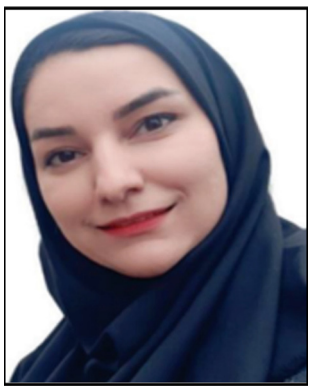

Elham Chamanehpour

Elham Chamanehpour received her B.Sc. Degree (2013) from Ferdowsi University of Mashhad and her M.Sc. Degree (2015) from the University of Birjand in Environmental Science, Iran. She is a Ph.D. candidate and is working on the synthesis of g-C_3N_4-engineered MOF for hydrogen production and carbon dioxide removal. Currently, she is a Visiting Researcher at Smart Materials, University of Southern Denmark, Sønderborg, and her main focus is the development of nanofibers for environmental remediation, renewable energy, catalysis, and biomedical applications.

Yogendra Kumar Mishra

Yogendra Kumar Mishra is Professor MSO at Mads Clausen Institute, University of Southern Denmark (SDU), Sønderborg, Denmark. Prior to SDU, he was leading a scientifically independent group as Functional Nanomaterials Chair, Institute for Material Science, Kiel University, Germany. He did his Habilitation in Materials Science at Kiel University in 2015 and PhD in Physics in 2008 at Inter University Accelerator Centre/ Jawaharlal Nehru University, New Delhi, India. At SDU Sønderborg, he is heading the 'Smart Materials' group with the main focus on the development of sustainable 3D nanomaterials for advanced technologies via *green transition. He has received prestigious awards, such as the Alexander von Humboldt Fellow, BHJ Fonden Denmark, and Fellow of the Royal Society (FRSC) of Chemistry UK. He has published over 350 research papers, which are cited over 20 000 times, with an h-index of over 76.*

Table 1 Polyaniline/chalcogen nanocomposites

Material	Synthesis process	Significant properties	Ref.
Se/PANI	Chemically doped by dissolving Se in chloroform in EB form of PANI	Electronic: DC conductivity	11
Se/PANI	Se pellets added in PANI EB solution in DMSO and heated	Optoelectronic	19
Se NW/PANI	Se nanowire is doped in swollen EB PANI by dissolving it in chloroform	Field emission	20
Se/PANI	Polymerized after mixing Se and aniline solution	Electronic: AC conductivity	21
G-Se/PANI	GO added during polymerization of aniline on Se nanowire	Electrochemical: discharge capacity	22
UIO-67@Se/PANI	Aniline polymerized on UIO-67@Se powder	Electrochemical: specific capacity	23
$Se_{0.95}Fe_{0.05}$/PANI	*In situ* polymerization	Optoelectronic: CIE coordinates, magnetization	24
Te/PANI/microporous phenolic foam	Galvanostatic deposition of Te on PANI-coated phenolic foam	Thermoelectric (TE)	25
Te/PANI	PANI EB doped with acidic solution of Te.	Electronic: DC conductivity	26
Te/PANI	Te-catalyzed polymerization of aniline using hydrazine hydrate, forming polyaniline-coated Te nanowire	Nonlinear optical (NLO) property	27
PANI/Te Nanorod	Te nanorod dispersion in m-cresol used for doping in CSA-doped EB PANI	Thermoelectric (TE)	28
PANI/Se-Te on LLC template	After potentiostatic polymerization of aniline Brij56 LLC template, mesoporous Se-Te layer was electrodeposited using Se-Te Brij56 LLC electrolyte	Electrochemical	29
PANI/SWNT/Te	Aniline *in situ* polymerized with SWNT, and Te attached hydrothermally later	Thermoelectric	30
(MWCNTs)-Te nanorod/PANI	Te and MWCNT dispersed in m-cresol ultrasonically and mixed with PANI–*m*-cresol solution	Thermoelectric, transport parameters	31
PANI/Te	Following 28	Thermoelectric	32
Te_xS_y/polyaniline	Single-step nonlinear electrochemical method	Electrochemical Impedance	33
Te/PANI	Te incorporated in PANI solution	Electrochemical, charge-transport mechanism	34
Te/PANI	*In situ* polymerization of aniline with tellurium	EMI shielding	36

Pawan K. Khanna

Pawan Kumar Khanna received his PhD in Organometallic Chemistry of Se & Te from the Indian Institute of Technology (IIT), Bombay in 1990. He went to Queens' University of Belfast and University of Wales at Swansea (UK) for post-doctoral studies with Prof. Christopher P Morley during 1989–1992. He was awarded the BOYSCAST Fellowship of DST, Govt of India, during 1998–1999 to work on quantum dots at the University of St. Andrews, Scotland (UK), with Professor David J Cole-Hamilton. He is currently a Senior Professor in the Dept. of Applied Chemistry at the Defence Institute of Advanced Technology (DIAT), Pune, India. His research interests include applied organometallic chemistry, materials chemistry, nano-chemistry, quantum dots, metal, chalcogenides and metal oxide nanomaterials for application in the areas of photonics, EMI shielding, photocatalysis, thermoelectric and biomedical sciences. He has published over 200 research papers with 10 patent applications and completed 20 research projects funded by Govt. agencies. He has guided over 100 graduate/post-graduate students including PhD/post-doctoral fellows. He has been named a top 2% scientist in the world for 4 consecutive years by the study conducted by researchers of Stanford University, USA. His current

2.1 Polyaniline/selenium (PANI/Se) nanocomposites

Chemical methods have been widely investigated for the synthesis of Se/PANI nanocomposite mostly employing two main approaches for doping Se in polyaniline, as follows:[11,19–21]

i. Mixing Se before polymerization in aniline solution and

ii. Doping Se in PANI EB solution after polymerization.

Each method significantly impacts the structural, electrical, and morphological properties of the resulting nanocomposite, making the choice of synthesis technique crucial. For instance, it has been demonstrated that PANI can be synthesized through the chemical oxidation of aniline using APS and its composite with Se on Si-substrate can be studied to understand the nature of the film in terms of the distribution of Se in the PANI matrix using time-of-flight secondary ion mass spectroscopy (TOF-SIMS).[19] This revealed a uniform distribution of selenium with both submicron dots and clusters, where the larger clusters have a higher concentration of Se than the average Se concentration (Fig. 1). These distribution patterns are crucial given that they influence the electronic

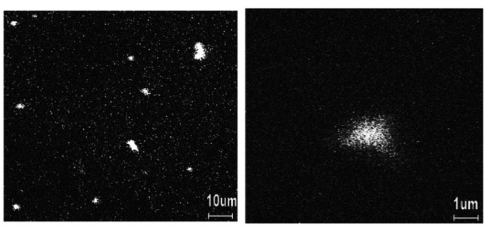

Fig. 1 TOF-SIMS image of Se distribution in PANI film. [Reproduced from ref. 19, with permission from Elsevier, Copyright 2003.]

and optical properties of the composite. Similarly, Shumaila *et al.*[20a] demonstrated that Se nanowires (45–75 nm diameter) prepared using SeO_2, β-cyclodextrin and vitamin C can be mixed with PANI EB ultrasonically in chloroform to form a PANI/Se nanocomposite. This composite exhibits potential in vacuum microelectronic devices and plastic display industries for field emission behaviour. Upon the application of a high electric field, electrons can be emitted by quantum tunnelling. This emission is dependent on the work function of the material and its field enhancement factor.[20b] Utilizing an *in situ* approach, Ozkazanc *et al.*[21] prepared a PANI/Se composite by mixing pre-dissolved selenium in nitric acid with aniline and APS, followed by spin coating. Their work highlighted a distinct FTIR peak at 872 cm^{-1} associated with the Se–Se stretching vibrations, indicating the successful incorporation of selenium in the polymer matrix. This method showed that by varying the concentration of selenium, the band gap and conductivity of the composite can be modulated, which it vital for optimizing materials for specific electronic applications such as transistors and diodes. Furthermore, the band gap can be engineered by the doping of Se in PANI *via* the doping process, which can be evaluated by optical measurement, and this doping can increase the conductivity by three orders of magnitude.[11] The initial morphology of the selenium nanoparticles may influence the morphology of the PANI/Se nanocomposite if the composite is generated *via ex situ* processing, whereas *via in situ* processing, the morphology can be controlled by the reaction parameters and the reagents employed to generate selenium.

Overall, doping with spherical Se particles led to the formation of granular cluster structures, whereas upon doping with Se nanowires, a fibrous interwoven morphology was observed by researchers. It was believed that this arrangement may provide effective conductive pathways due to the movement of delocalized electrons along the conjugated pathways and the electron hopping mechanism between the adjacent redox sites within the polymer chain. The FTIR spectra showed the presence of structural changes in PANI after Se doping and provided evidence for the interaction between Se and the polymer chain. It has been suggested that due to the electrostatic interaction between the nitrogen atoms and selenium ion, the physical adsorption of Se on the PANI molecule is also possible.[21]

Researchers have also investigated field emission behaviour of PANI/Se nanocomposites using an in-house fabricated setup at room temperature, maintaining a pressure of 10^{-6} Torr in the vacuum chamber. It was observed that 10% (w/w) Se doping showed the highest emission characteristics with a low turn-on field of 1.2 V m^{-1}, making it promising material for field emission-based applications.[20a]

Moreover, novel composites such as graphene/Se/PANI have been reported to show a superior performance in Li-ion battery applications and displayed improved cycling durability and excellent performance at high rates, demonstrating a reversible discharge capacity (after 200 cycles) of 567.1 mA h g^{-1} at 0.2 C and 510.9 mA h g^{-1} at 2 C.[22] The robust electrochemical performance of this nanocomposite demonstrates its potential as a cathode material for Li–Se batteries. Another innovative approach by Ye *et al.*[23] involved creating a UIO-67@Se/PANI composite for Li–Se batteries using Zr-based metal–organic frameworks (MOFs) coated with PANI. This composite demonstrated significant specific capacities and retention rates, highlighting the versatility of Se/PANI composites in energy storage applications. Specifically, it achieved a notable specific capacity of 248.3 mA h g^{-1} at 1 C after 100 cycles, while maintaining a capacity of 203.1 and 167.6 mA h g^{-1} at higher rates of 2 C and 5 C, respectively. Heiba *et al.*[24] conducted the synthesis of polyaniline (PANI) combined with $Se_{0.95}Fe_{0.05}$ at different weight ratios (5% and 10%) using an *in situ* polymerization technique. Analysis using XRD verified the structural properties of PANI and the presence of $Se_{0.95}Fe_{0.05}$. It indicated that PANI possessed a semi-crystalline structure and the appearance of $Se_{0.95}Fe_{0.05}$ in two phases (trigonal-Se and orthorhombic-$FeSe_2$) in the PANI nanocomposites (Fig. 2). The nanocomposites exhibited weak ferromagnetic behaviour, with enhanced coercivity and saturation of magnetization with an increase in the weight percentage of $Se_{0.95}Fe_{0.05}$ in PANI.

The synthesis and characterization of selenium/polyaniline (Se/PANI) nanocomposites offer exciting insights for their diverse applications. Se doping in PANI has been achieved through methods such as chemical oxidation and *in situ* polymerization, influencing its electrical, morphological, thermal, structural and optical properties. These nanocomposites show promise in fields such as electronic devices, field emission applications, and energy storage systems. Future research avenues should focus on fine-tuning the synthesis approaches, understanding the fundamental interactions between Se and PANI, exploring their performance in practical devices, and optimizing their properties for enhanced functionality and sustainability. Additionally, investigating novel composite architectures and exploring their applications in emerging technologies such as Li-ion batteries and environmental remediation can further expand the scope of Se/PANI nanocomposites. Furthermore, it is possible to propose that Se/PANI nano-composite can act as precursors of Se for the preparation of metal selenide QD/PANI nanocomposites.

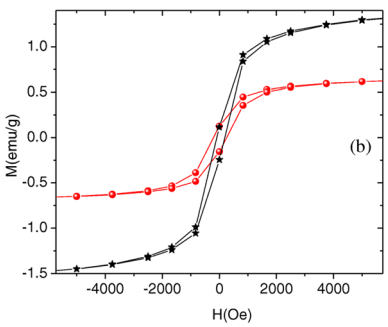

Fig. 2 Room temperature magnetization curves of PANI/$Se_{0.95}Fe_{0.05}$ (5 wt% in black and 10 wt% in red) nanocomposites. [Reproduced from ref. 24, with permission from Springer, Copyright 2019.]

2.2 Polyaniline/tellurium (PANI/Te) nanocomposites

The global energy crisis necessitates innovative energy solutions, which often depend on the use of technologically advanced polymer-composites materials given that they are highly suitable for a range of energy applications including thermoelectric (TE) technologies, offering environmentally friendly and cost-effective means to convert low-grade heat into electricity. In this section, we explore the synthesis and characterization of PANI/Te hybrid films and the studies on their thermal, electrical and optical properties. To date, several methods have been adopted by researchers for the preparation of PANI/Te nanocomposites. One of the methods involved the electrodeposition of a Te film above PANI-coated phenolic foam. Alternatively, the other method involved the use of an acidic aq. solution of Te and its reaction with PANI for the fabrication of a PANI/Te nanocomposite. It was reported that the Te film could be electrodeposited onto phenolic foam using PANI coatings as conducting transition layers.[25] The structural and thermoelectric behaviour of the deposited films exhibited uniformity and preferred crystal orientation along the *c*-axis direction.

Thermopower measurements revealed the maximum value of 342 μV K^{-1} at 473 K, showcasing the thermoelectric potential of the nanocomposites. Kazim *et al.*[26] reported the doping of PANI with varying Te concentrations to improve the electrical properties of the composite. The maximum dc conductivity was found to be 6.635×10^{-5} Ω^{-1} cm^{-1} for 25% Te doping. It was discussed that Te^{2+} doping resulted in carrier delocalization due to the attraction between neighbouring polymeric units arising from the incorporation of Te in the PANI chain. This arrangement led to the formation of polarons and bipolarons, thus enhancing the carrier mobility with an increase in the doping level of Te^{2+}. Also, varying the doping concentration to achieve useful properties was discussed.

It was proposed that the electron delocalization in the composite occurs due to the presence of dopant and sulfuric acid together, which perhaps act as double doping reagents.[26] In another synthesis process, Te was freshly prepared using H_2TeO_3 *via* hydrazine hydrate and was used as a catalyst in the polymerization of aniline to prepare PANI-coated Te nanowires, where the broom-shaped hierarchical structure demonstrated superior NLO behaviour in comparison to its individual components according to the discussion by the authors.[27] Wang *et al.*[28] employed an ultrasonic dispersion method to form a Te/PANI film, which exhibited an enhanced thermoelectric figure of merit (zT). This film showed a power factor of 146 μW mK^{-2} and its zT was enhanced from 0.156 at room temperature to 0.223 at 390 K. A nanocomposite with a chalcogen alloy, *i.e.*, PANI/Se–Te nanocomposite, was synthesized[29] *via* electrodeposition on a Brij56 (surfactant) lyotropic liquid crystalline (LLC) template and studied.

The integration of polyaniline (PANI) with tellurium (Te) in nanocomposites presents a promising avenue for enhancing its thermoelectric (TE) application. It was mentioned that synthesized PANI/Te hybrid films exhibited improved thermoelectric properties according to their characterization, owing to their well-matched nanoscale interfaces, enhanced carrier transport, and low thermal conductivity. Wang *et al.*[30] employed an innovative approach for the *in situ* synthesis of water-soluble ternary PANI/SWNT/Te (polyaniline/single-walled nanotube/tellurium) nanocomposites, showing uniform structures and remarkable thermoelectric (TE) properties. The nanocomposite films demonstrated exceptionally high Seebeck coefficients, which was ascribed to the energy filtering action by PANI/SWNTs together with the PANI/Te interfaces, maintaining a good balance between electrical and thermal conductivity (0.2 to 0.4 W m^{-1} K^{-1}) with the TE power factor reaching 101 μW m^{-1} K^{-2}, surpassing that of the individual components present in the composite (Fig. 3). The presented approach opens possibilities for designing high-performance ternary organic–inorganic composite TE materials with various fillers.

In another study, interfacial engineering was employed[31] to intelligently craft Te-based ternary hybrid nanomaterials using tellurium nanorods, MWCNTs and PANI. The interactions among MWCNTs, Te nanorods and PANI lead to the formation of well-bonded interfaces, enhancing the electrical conductivity and thermopower simultaneously. The optimized composition resulted in a power factor of 54.4 μW m^{-1} K^{-2} (Fig. 4). This research offered a technically improved approach for enhancing the thermoelectric performance of conducting polymer-based hybrids, showing promise for economical flexible energy conversion devices suitable for large-scale production.

Further research in this field was continued by Wang *et al.*,[32] where they directed their attention towards enhancing

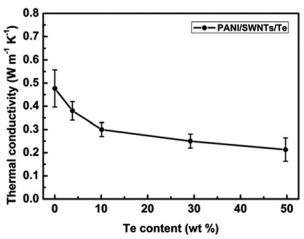

Fig. 3 Variation in thermal conductivity with Te content in PANI/SWNT/Te nanocomposite. [Reproduced from ref. 30, with permission from The Royal Society of Chemistry, Copyright 2017.]

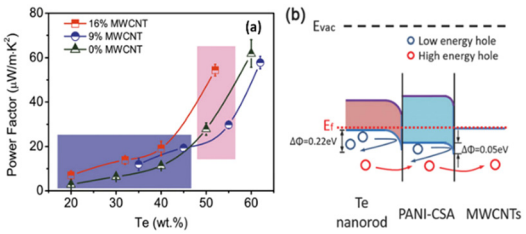

Fig. 4 (a) Comparison of TE properties and (b) interfacial energy filtering effects. [Reproduced from ref. 31, with permission from Wiley VCH, Copyright 2018.]

the carrier concentration by subjecting polyaniline/Te nanorod hybrid films to thermal treatment. The outcome demonstrated that thermal treatment effectively tuned the carrier concentration, leading to a notable enhancement in thermoelectric electric performance. This study revealed that the hybrid film produced at 180 °C exhibited a 20% increase in power factor compared to the original film by controlling the dopant quantity and carrier concentration *via* thermal processing. A cathode material for Li-ion batteries with high conductivity and capacity was discussed by Li *et al.*,[33] showing the potential of tellurium in this field. This Te-containing PANI composite exhibited a large initial capacity and maintained cycling stability at 5 A g^{-1}, suggesting a sustainable strategy for battery fabrication. The approach and designed nanorod structure presented a promising solution to the challenges associated with tellurium-based batteries. Rani *et al.*[34] fabricated a Te/PANI nanocomposite *via* the solid-state chemistry method by blending varying concentrations of Te (5%, 10%, and 15%) that with PANI. The resulting composite displayed adaptability for various energy harvesting purposes, including both conversion and storage. The successful integration of Te in the matrix at the benzenoidal functionality, with oxygen bonding *via* sulphonated disorder contributed to the super-capacitive behaviour. The authors concluded that 10% Te concentration was optimal for achieving both photo- and electrochemical conduction performance.[35] Recently, it was demonstrated that the PANI/Te nano-composite can be the future EMI shielding materials for blocking electromagnetic waves/radiations in the X-band. It was hypothesized that the composite, which initially had low conductivity, could be converted to a reasonably higher conducting material by doping with silver and excess Te. The authors showed that the EMI shielding efficiency of the composite was about −10 dB due to the presence of *in situ*-generated TeO_2.[36] Thus, the exploration of PANI/Te nanocomposites for applications beyond thermoelectricity, such as energy storage and photoconduction, holds significant potential, paving the way for multifunctional and versatile conducting polymer-based materials for diverse energy applications. Furthermore, the development of ternary PANI/SWNT/Te and PANI/MWCNTs-Te nanocomposites demonstrated the feasibility of incorporating multiple components to tailor properties, highlighting avenues for designing high-performance organic–inorganic hybrid materials with enhanced functionality and versatility (Fig. 5).

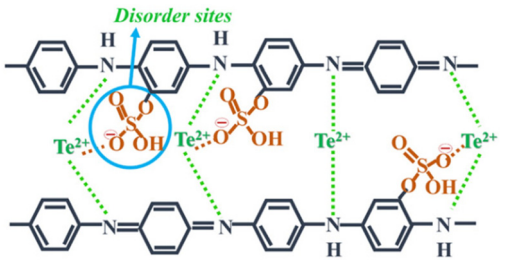

Fig. 5 Charge transport mechanism in Te-PANI. [Reproduced from ref. 34, with permission from Springer Nature, Copyright 2023.]

3. PANI–metal chalcogenide nanocomposites

The research on polymer-based thermoelectric composites, focusing on polyaniline (PANI) and inorganic nanoparticles such as ZnSe, CdSe, CdTe, PbTe, Bi_2Se_3, Bi_2Te_3, Ag_2Se, and $Bi_{0.5}Sb_{1.5}Te_3$, as well as mixed metal chalcogenides provides valuable conceptual insights into enhancing the thermoelectric performance through tailored nano-structuring and interface engineering. By incorporating these nanoparticles in PANI matrices through diverse synthesis methods, such as solvothermal, electrodeposition and chemical oxidation methods, researchers have achieved significant improvements in electrical conductivity, Seebeck coefficient and power factor. The utilization of low-dimensional nanostructures and introduction of hybrid interfaces in PANI-based composites have demonstrated promising results in enhancing the thermoelectric properties, paving the way for potential applications in flexible thermoelectric devices and low-temperature thermoelectric systems. Future research in this domain can focus on further optimizing the nano-structuring process, exploring novel synthesis techniques and elucidating the underlying mechanisms governing the enhanced thermoelectric performance. Additionally, investigating the scalability, long-term stability, and environmental effects of PANI-based thermoelectric composites will be crucial for their practical implementation in energy harvesting and waste heat recovery applications. In this section, we present a summary of the research on PANI-chalcogenide nanocomposites. Polyaniline-chalcogenide nanocomposites have also been reported as potential electronic materials.[36–45] Researchers adopted a variety of methods for their synthesis and the fabrication of films of these composites, which are described in Table 2. Selected metal selenides and tellurides are discussed in subsequent sections.

3.1. PANI/zinc chalcogenides

According to our extensive literature search, we could not find any reports on ZnTe/PANI composites; however, there are a few reports emphasizing the incorporation of ZnTe in other polymers. Thus, considering this lack of information, only ZnSe/PANI is discussed here. However, this implies that researchers can focus on these materials and conduct extensive research to expand the utility of ZnTe in electronic and photonics application. Bormashenko *et al.*[46] conducted research on utilizing films of ZnSe and polyaniline emeraldine base (PANI EB) as coatings to reduce the reflection in the near and mid-infrared (NIR and MIR) optical regions (Fig. 6). The PANI coating effectively minimized the Fresnel losses in the middle and near IR regions, *i.e.*, wavelength range of 1.0–6.25 μm. The investigation also assessed the damage threshold of the coating under laser irradiation at a wavelength of 1.5 μm, indicating that ZnSe has satisfactory microhardness when coated. Thus, thin PANI EB layers are well-suited for coating infrared (IR) optics elements due to their broad IR transparency, high IR

Table 2 Some polyaniline/metal chalcogenide nanocomposites

Material	Synthesis process	Significant properties	Ref.
CdSe/PANI	Aniline and CdSe NPs were mixed by ultrasonication, and then polymerized by APS	Electronic: conductivity, current density	5
C_{60}/CdSe/PANI	C_{60}/CdSe was used as a promoting agent for the polymerization of aniline	Optoelectronic & thermoelectric	37
PANI/CdSe (TPs)	PANI film was dipped in CdSe solution for a few seconds	Optical: PL	38
Cu_2Se/PANI	In aniline, HCl solution of Cu_2Se NPs was mixed and polymerized by APS	Optical and electronic	39
PANI-Ag_2Se/PVDF	PANI layer was coated over Ag_2Se using dodecylbenzene sulphonic acid	Thermoelectric	40
PANI-Bi_2Se_3	Template-based *in situ* oxidative chemical polymerization by APS after mixing 30% Bi_2Se_3 NPs in aniline solution	Thermoelectric	41
PANI-Bi_2Te_3	Bi_2Te_3 nanorod in aniline-SSA solution, then APS added for polymerization	Thermoelectric	42
Bi_2S_3/PANI and Bi_2Te_3/PANI	Chalcogenides were sonicated in toluene. Then PANI was added and heated with intermittent sonication	Thermoelectric	43
PbTe-PANI core–shell	*In situ* fabrication by dissolving APS in PbTe precursor solution and mixing in aniline-CCl_4 solution for interfacial polymerization	Thermoelectric	44
PANI/$Cu_2ZnSnSe_4$	PANI was electrodeposited on fluorine doped tin oxide (FTO)/glass electrode. Then CZTSe was electrodeposited on it using aqueous electrolyte solution of its precursors in tartaric acid solution	Electronic: current density, photocurrent	45
CdTe/PANI	Galvanostatic electrodeposition of PANI on ITO and CdTe doping by soaking solution	Optoelectronic: electroluminescence (EL)	46
CdSeTe@PANI	To CdSeTe QDs, HCl and aniline were added, which was polymerized by adding $K_2S_2O_8$	bioimaging	47*a*

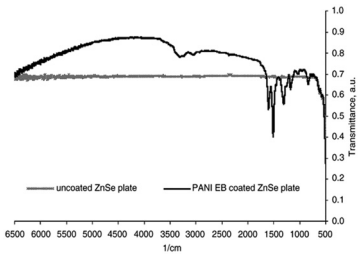

Fig. 6 Comparison of coated and uncoated ZnSe plates. [Reproduced from ref. 46, with permission from Elsevier, Copyright 2004.]

radiation stability, high optical tolerance, and good surface hardness. These properties make them ideal for various IR optics applications, including antireflective coatings for IR windows and lenses.

Kaushik *et al.*[47*a*] presented findings regarding the creation of diffused polyaniline (PANI)/ZnSe QD structures through the electrochemical method, with potential applications in LEDs. The polyaniline films formed ordered bundles of closely packed polymeric strands, allowing the uniform dispersion of ZnSe QDs. The resulting PANI/ZnSe films exhibited significantly improved luminescence.

The particle size of ZnSe QDs was 5 nm, which is smaller than the Bohr exciton radius for ZnSe (9 nm).[47*b*] This small size leads to a high density of surface states, which trap the photoexcited carriers, thereby suppressing the excitonic luminescence. However, when PANI is used as a host, it passivates these surface states, enhancing the luminescence of the composite material.

Shirmardi *et al.*[48] investigated the impact of incorporating polyaniline (PANI) on the photocatalytic efficacy of ZnSe NPs as an organic semiconductor. The co-precipitation method was used to synthesize pristine ZnSe NPs and core–shell ZnSe/PANI type-II heterojunction nanocomposites, thus separating the photogenerated electron–hole pairs, reducing their recombination and preparing them for photocatalytic application. The composite showed a reduced band-gap value compared with the pristine ZnSe NPs, which was induced by PANI, with a shift in its VB and CB edges. The photocatalytic assessments for the removal of methylene blue (MB) and chromate ions upon the action of visible-light showed the enhanced behaviour of the ZnSe/PANI nanocomposites compared to pure ZnSe NPs due to their type-II heterojunction. The results of the Brunauer–Emmett–Teller (BET) calculations highlighted a decrease in the textural properties of the nanocomposite due to PANI, such as its specific surface area, pore size and pore volume.

Shokr *et al.*[49] conducted a study on the synthesis of nanocomposites comprised of polyaniline and ZnSe, wherein ZnSe nanoparticles, approximately 8.5 nm in size, were produced *via* the colloidal technique, while polyaniline was synthesized together with the ZnSe nanostructure. The XRD analysis revealed the semicrystalline nature of polyaniline and cubic crystal structure of ZnSe. The SEM images illustrated an enlargement in particle size due to the integration of ZnSe in the polyaniline matrix. UV-Visible spectroscopy was employed to examine the optical characteristics of the nanocomposites, revealing a reduction in the energy gap of polyaniline by about 0.5 eV with an increase in Zn content. Overall, E_g was enhanced from 3.42 to 2.92 eV. ZnSe, being a semiconductor with a wide bandgap, introduces additional electronic states with a lower activation energy within the band structure of PANI. These states can facilitate the generation of more holes due to the increase in dc conductivity. Specifically, the interaction between the PANI matrix and ZnSe quantum dots can lead to the hopping of the charge carriers, where the electrons from PANI can be transferred to ZnSe, leaving behind holes in PANI. This charge transfer process effectively increases the

hole concentration in polyaniline. The thermoelectric power measurements suggested that holes were the predominant carriers, exhibiting increased mobility and quantity, together with a reduced potential barrier with an increase in the ZnSe concentration within the polyaniline matrix. Jijana *et al.*[50] produced electrochemically polymerized ZnSe quantum dot/PANI nanofiber composites having a 3-mercaptopropionic acid-capping on ZnSe. It was reported that the quantum dots were attached to PANI through the carboxylic acid functionality, thus maintaining the functionalities of both PANI and QD surface, enabling the attachment of horseradish peroxidase (HRP) enzyme, a bio-receptor. Subsequently, a biosensor was constructed using this composite, which showed excellent capacity to detect 17β-estradiol under different conditions. The explored research on polyaniline (PANI) and zinc selenide (ZnSe) nanocomposites provides valuable conceptual insights into their multifaceted applications.

The utilization of PANI as an antireflection coating for infrared optical elements, in combination with ZnSe, demonstrates its potential to mitigate Fresnel losses and transmit high power density infrared radiation. The creation of PANI/ZnSe through electrochemical methods reveals promising prospects for enhancing the luminescence in LED applications and biosensing. The incorporation of PANI as an organic semiconductor in ZnSe nanoparticles significantly improves their photocatalytic efficacy, opening avenues for environmental remediation. Additionally, the synthesis of PANI/ZnSe nanocomposites with tailored properties, such as semicrystalline structures and altered optical and electrical characteristics, shows potential in thermoelectric applications. Looking forward, there is future scope in optimizing synthesis techniques, ensuring scalability, and exploring the long-term stability of these nanocomposites. Further research should delve into integration of these materials in practical devices, understanding their performance under diverse conditions and investigating their environmental impact. Novel combinations of conducting polymers and semiconductors, together with the development of multifunctional nanocomposites, can expand the horizon of applications in electronics, sensors, and beyond, paving the way for technological advancements and real-world implementations.

3.2. PANI/cadmium chalcogenides

Singh *et al.*[5] mixed CdSe in aniline, and then polymerized it using APS, which exhibited an increase in current density by three orders compared to pure PANI. The observed ohmic behaviour in the forward bias voltage was attributed to the conduction behaviour exhibited by the free charge carriers, specifically "polarons and bipolarons".

The prominent presence of cubic phase CdSe was examined with a slightly lower lattice constant value of 0.554 nm. The short circuit current density was found to increase to 150 A cm^{-2}. Thus, the increase in the conductivity of the nanocomposite makes it suitable for applications in p-n junction diodes, sensing devices, *etc*. Joshi *et al.*[35] reported the fabrication of heterojunctions employing electro-chemically deposited PANI and CdX (X = S, Se, Te) thin films. The ideality factors and flat band potentials were determined for CdS, CdSe, and CdTe-based junctions, indicating their suitability for optoelectronic applications. Their heterojunction and diode properties, *e.g.* current, and capacitance voltage, *i.e. I–V* and *C–V*, were studied.

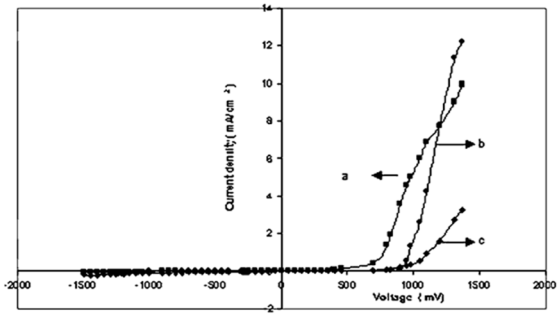

Fig. 7 Current density v/s voltage (a) CdS/polyaniline, (b) CdSe/polyaniline, and (c) CdTe/polyaniline. [Reproduced from ref. 35, with permission from Springer, Copyright 2007.]

Fig. 7(a–c) display the *I–V* characteristics of the junction between cadmium chalcogenide and polyaniline. It was shown that CdX/polyaniline can function as diode materials. Not only tellurium-based II–VI semiconductors but also selenium-based semiconductors play a vital role in the development of these composites for photovoltaics. Ahilfi *et al.*[51] synthesized PANI-based nanocomposites employing CdSe nanoparticles through a chemical and electrospinning method, where the crystalline cubic CdSe/PVA nanocomposite served as the acceptor, while amorphous PANI-DBSA/PS nanofibers acted as the donor in a hybrid solar cell. Also, the fine dispersion of PANI within the PS film can generate photogenerated electrons and holes when exposed to UV light, resulting in an increase in absorption in the near UV range. Patullo *et al.*[52] attempted to enhance the photovoltaic conversion efficiency *via* the utilization of highly conductive materials such as PANI and (PEDOT:PSS) by employing the dip-coating technique on a pulsed layer-deposited CdS/CdTe film as the substrate.

This studied showed that the electrochemically synthesized PANI/CdTe composite on ITO exhibited superior anticorrosion properties to the pure polyaniline coatings on stainless steel (XC 70) due to the higher tendency of the protonated polyaniline to attract electrons, as revealed by the electrochemical impedance spectroscopic technique.[53]

Incorporating fullerene with PANI has also attracted attention from researchers and a study was undertaken by Rusen *et al.*,[37] who introduced a new technique to oxidatively polymerize aniline (PANI). They developed a method that employed fullerene C_{60}/CdSe QDs to enhance the polymerization process. This study also proposed the mechanism for the polymerization process, involving donor–acceptor exchange between the components based on their HOMO–LUMO energy levels, as shown in Fig. 8. This was an interesting study, where size-dependent polymerization was discussed, showing an increase in the polymerization efficiency with a decrease in the

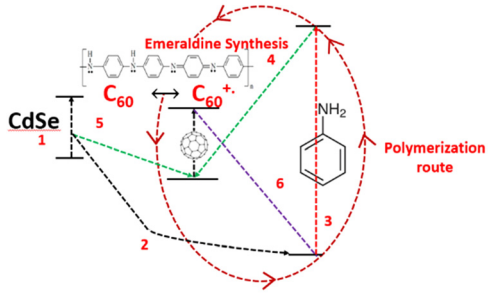

Fig. 8 Oxidative polymerization of aniline using CdSe-C_{60} system. [Reproduced from ref. 37, with permission from Nature, Copyright 2016.]

particle size of CdSe. CdSe tetrapods synthesized by the solvothermal method were incorporated in a PANI film *via* a low-cost chemical bath deposition method by Bhand *et al.*[38] to create void-free, densely packed, granular hybrid PANI/CdSe nanocomposite layers.

Enhanced absorption and photoluminescence (PL) intensities were observed in the visible to near-infrared (NIR) spectrum by increasing the dipping time. This augmentation can be attributed to the interaction between CdSe and the protonated N–H group of PANI. It was shown that the thermal stability was enhanced by the presence of CdSe in the nanocomposite compared to pure PANI. In another method, Gaponik *et al.*[54] applied galvanostatic electrodeposition to deposit polyaniline/CdTe nanocomposites on an ITO/glass substrate using colloidal CdTe and compared its photoluminescence and electroluminescence spectra, observing a peak at the same wavelength of 500 nm (Fig. 9) due to the size-dependent colour tunability from green to red. An increase in current was observed at a lower voltage in CdTe/PANI than CdTe. It was discussed that because of the better hole transporting property of polyaniline, the CdTe/PANI layer composites showed better a electroluminescence (EL) quantum efficiency. Xue *et al.*[55] observed a 40 times enhancement in fluorescence by polymerizing aniline on the surface of CdSeTe

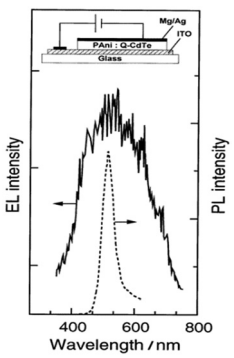

Fig. 9 PL and EL spectra of CdTe/PANI heterojunction. [Reproduced from ref. 54, with permission from The Royal Society of Chemistry, Copyright 1999.]

quantum dots. Also, it showed a high-amplified signal for cell imaging given that the fluorescence intensity was increased by a thousand times at the emission wavelength of 450 nm when incident with 360 nm light. They observed that when the CdSeTe QDs were capped by PANI, then the surface traps were passivated and the absorption and emission bands were blue-shifted. The absorption band shifted from 360 nm to 300 nm and the emission band shifted to 450 nm from 560 nm. The characteristic IR bands of the CdSeTe quantum dots were located at 1307 cm^{-1} and 1275 cm^{-1}. The interaction of the amine and carboxylic groups in PANI and the quantum dots caused a shift in the characteristic peaks of PANI. This study also showed that the CdSeTe/PANI composite was more negatively charged, where the zeta potential values of CdSeTe and CdSeTe/PANI QDs were found to be −29.9 mV and −53.1 mV, respectively.

Joshi *et al.*[56] reported the fabrication of an LPG sensor at room temperature (300 K), which was formed by a n-CdSe/p-polyaniline junction through the electro-chemical deposition method. The forward biased current–voltage characteristics displayed a significant shift for different LPG concentrations. The peak response, reaching up to 70%, was attained with a concentration of 0.08 vol% LPG. Similarly, in another study they investigated the response of an electrodeposited n-type CdTe and p-type polyaniline heterojunction for sensing liquefied petroleum gas at elevated temperature with notable response characteristics at a fixed voltage of +1.38 V for a response time ranging from 80 to 300 s and recovery time of about 600 s depending on the gas concentration.[57] Hybrid polyaniline (PANI) thin layers with CdTe, CdSe, and a combination of both NPs were fabricated by Verma *et al.*[58] using the spin-coating technique, where the chemical oxidation method was used for the preparation of PANI, while the solvothermal method was employed for the synthesis of CdTe and CdSe nanoparticles.

The absorption spectra revealed the formation of charge transfer complexes in the hybrid films, which was consistent with the cyclic voltammetry studies. There was another interesting study by Manaf *et al.*,[59] who incorporated PANI in glass/FTO/CdS/CdTe/Au diode structures, which exhibited enhanced photovoltaic activities, particularly open circuit voltage and fill factors. They suggested that PANI, synthesized through electrochemical methods, holds promise given that it is highly efficient and economical, resulting in relatively stable inorganic/organic hybrid thin layered solar cells. Also, Junior *et al.*[60] investigated the impact of incorporating polyaniline (PANI) at the junction of CdTe/CdS layers in hybrid solar cells with improved layer contact. The addition of PANI altered the cell characteristics, *e.g.* the open circuit voltage increased to 0.67 V, current density to 0.3 mA cm^{-2}, and the overall efficiency improved to 0.15%. Overall, it has been realized that binary chalcogenide semiconductors together with conducting polymers can become futuristic and alternate materials for energy application.

Xu *et al.*[61] suggested that the presence of oxide can enhance the electron transport. They developed a two-step

in situ emulsion method to generate a TiO_2 nanosheet/CdSe/polyaniline/graphene composite for *in situ* coating on to stainless steel (304SS) for photocathodic protection, which improved the electron transfer and cathodic protection efficiency. According to this study, the photoelectrochemical performance was significantly boosted due to the simultaneous effect of three factors, *viz.* broadened absorption range, effective separation of electrons and holes, and presence of a good conductive network.

Semiconductor/conducting polymer hybrid composites can also be effectively exploited for biomedical sensing applications. For example, in the study Liu *et al.*,[62] they focused on creating a photoelectrochemical (PEC) aptasensor to identify carbendazim (CBZ), a harmful substance found in pesticide residues, in tomatoes. The CdTe-PANI/MoS_2 heterostructure was shown to enhance the performance of the PEC aptasensor. It was demonstrated by the authors that the PEC aptasensor functioned in the "signal-off" detection mode, where the binding of the aptamer (specific nucleic acids) to CBZ on the surface of CdTe-PANI@MoS_2 hindered electron transfer.

The extensive investigations into polyaniline (PANI) composites with cadmium selenide (CdSe) and cadmium telluride (CdTe) nanoparticles revealed their versatile applications in electronic and optoelectronic devices. These studies demonstrated their enhanced electrical conductivity, improved photovoltaic activities, and significant potential in various applications such as p–n junction diodes, gas sensors, and solar cells. The incorporation of CdSe and CdTe nanoparticles not only contributes to an increase in current density and conductivity but also influences the optical properties, allowing for tunable colour emissions.

Similar to binary semiconductor/PANI hybrids, there is also good scope to combine ternary and quaternary semiconductors with conducting polymers and exploiting for a variety of sensing and energy applications. In this regard, the electrodeposition technique was employed to synthesize copper zinc tin selenide, *i.e.* CZTSe/PANI.[45] It was further stated that first PANI layer was deposited in potentiostatic mode on an FTO/glass substrate followed by the electrodeposition of CZTSe, resulting in a 20 times increase in photocurrent compared with CZTSe on FTO/glass alone.

The future scope lies in refining the synthesis techniques, optimizing the properties of nanocomposite, and exploring their integration into scalable devices. Further research avenues include investigating their long-term stability, environmental impact, and exploring novel combinations of polymers and different semiconductors for innovative applications in emerging technologies. The potential for tailored nanocomposites with superior performance suggests a promising future for PANI/CdSe/CdTe in diverse electro-, opto- and electronic applications.

3.3. PANI/bismuth chalcogenides

Polyaniline/Bi_2Se_3 nanoplates were synthesised *via in situ* solvothermal polymerization by Mitra *et al.*,[41] where the 2D layered structure showed an enhancement in carrier transport properties through the hopping model. The power factor of the composite was reported to be 30 times higher than that of pure PANI with 30% Bi_2Se_3 content. Subramanian *et al.*[63] investigated the electrodeposition process of thin layers of Bi_2Se_3 and Bi_2Se_3 films doped with polyaniline (PANI). The optical band gap energy of the initially deposited Bi_2Se_3 thin film increased with an increase in the concentration of PANI. Electrical conductivity assessments revealed Arrhenius behaviour across all the films, with PANI-dependent activation energies. Reddy *et al.*[43] reported the synthesis of Bi_2Te_3 by reacting bismuth oleate and trioctylphosphine telluride (TOP-Te) at about 80 °C. Subsequently, polyaniline was coated on it by refluxing in toluene-dispersed polyaniline at about 100 °C. The as-prepared Bi_2Te_3 nanorods were coated with PANI to improve their thermoelectric properties. Likewise, Chatterjee *et al.*[64] synthesized a PANI/Bi_2Te_3 composite simultaneously employing an electrochemical and deposition method to obtain rod-like nanostructures with a diameter of less than 100 nm. The UV–Vis spectra demonstrated the degree of doping in the nanocomposite.[42] The broad band at around 634 nm originally present in polyaniline disappeared in the spectrum of the nanocomposite, indicating organized molecular arrangement along the nanorod axis, which diminished the π–π* conjugation imperfections within PANI. Likewise, Yadav *et al.*[36] recorded the UV-Vis spectra of a PANI/Te nanocomposite in DMF, depicting π–π* at 354 and polaron–π* transitions at wavelengths of 382 and 602 nm, respectively (Fig. 10). The thermoelectric power (S) of the PANI/Bi_2Te_3 composite changed due to the change in charge carriers from holes to electrons. A core–shell nanocable design composed of PANI/Bi_2Te_3 was developed using a solvothermal and chemical oxidative process to obtain lower thermal conductivity, leading to a higher thermoelectric power above 380 K.[42]

Guo *et al.*[65] explored the enhancement in the thermoelectric power of polymer-based composites through carrier energy-filtering action at the hybrid organic–inorganic interface. $Bi_{0.5}Sb_{1.5}Te_3$ nanoplates (BST NP) were incorporated in camphor-sulfonic acid-doped polyaniline (CSA:PANI) *via* cryo-

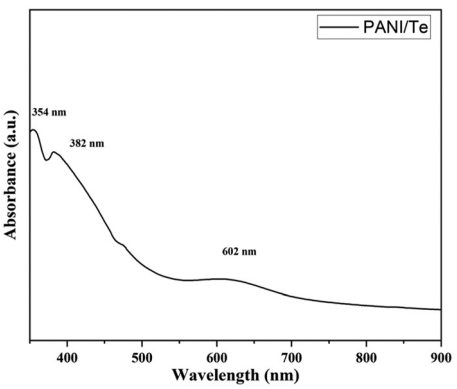

Fig. 10 UV-Visible spectrum of PANI/Te in DMSO. [Reproduced from ref. 36, with permission from The Royal Society of Chemistry, Copyright 2023.]

genic grinding and hot pressing, which formed abundant hybrid interfaces in the CSA:PANI/BST NP composites. This configuration increased the Seebeck coefficient and power factor substantially, which was attributed to the energy-filtering effect at the CSA:PANI/BST NP interface.

Consequently, the zT values reached 8.637×10^{-4} at 300 K and 1.64×10^{-3} at 400 K. The enhanced thermoelectric properties demonstrated the effectiveness of the energy-filtering action in TE materials fabricated using PANI, marking a significant advancement in this field. Similarly, Zhmurova *et al.*[66] developed emeraldine salt-type PANI-based nano-thermoelectric materials incorporating Te^0 and Bi_2Te_3 nanoparticles together with multi-walled carbon nanotubes (MWCNT). This study investigated the temperature-dependent direct current (DC) electrical conductivity of the nanocomposites in the temperature range of 298–353 K. Generally, an increase in the inorganic nanophase content boosted the conductivity of the ES-PANI/Te^0 and ES-PANI/Bi_2Te_3 nanocomposites.

Hegde *et al.*[67] studied the thermoelectric (TE) performance of composites consisting of $(Bi_{0.98}In_{0.02})_2Te_{2.7}Se_{0.3}$/PANI and $(Bi_{0.98}In_{0.02})_2Se_{2.7}Te_{0.3}$/PANI in the temperature range of 10 to 350 K. The BIS/PANI composite exhibited a six-fold decrease in electrical resistivity compared to the BIT/PANI sample. The zT value of BIT/PANI was shown to increase by 20 times compared to the pure BIT samples, suggesting that it is a potential candidate for low-temperature TE applications. Studies on polyaniline (PANI) composites with bismuth chalcogenides (Bi_2Se_3, Bi_2Te_3, and $Bi_{0.5}Sb_{1.5}Te_3$) revealed significant improvements in thermoelectrics. For instance, PANI/Bi_2Se_3 composites showed a 30-fold increase in power factor, suggesting future advancements in flexible thermoelectric generators. Doping Bi_2Se_3 in PANI enhances its optical and electrical properties, making it suitable for high-efficiency optoelectronics. PANI-coated Bi_2Te_3 and PANI/Te composites showed an improved thermoelectric performance, with potential applications in waste heat recovery and space technology. Incorporating $Bi_{0.5}Sb_{1.5}Te_3$ into PANI increased its Seebeck coefficient, making it useful for microelectronics energy harvesting. These materials also exhibit enhanced conductivity for high-sensitivity sensors and flexible electronics. Future research should optimize the synthesis and explore the charge dynamics of these composites and integrate them in advanced energy storage and environmental monitoring devices.

3.4. PANI/silver chalcogenides

Park *et al.*[40] synthesised PANI-Ag_2Se/PVDF composite films through a one-step method, employing electrochemical deposition (Fig. 11), where the nanocomposites were investigated with varying PANI coating cycles to enhance their electrical conductivity with a decrease in Seebeck coefficient. The improved power factor with stable performance even after 1000 bending cycles demonstrated the excellent flexibility of the nanocomposites. When used in a thermoelectric device, the nanocomposite generated an output voltage and power in a variable temperature range (ΔT), indicating the possibility of its application in flexible thermoelectric applications. In another study, core/shell-type Ag_2Te/PANI nanostructures were successfully synthesized using a one-pot interfacial method.[68]

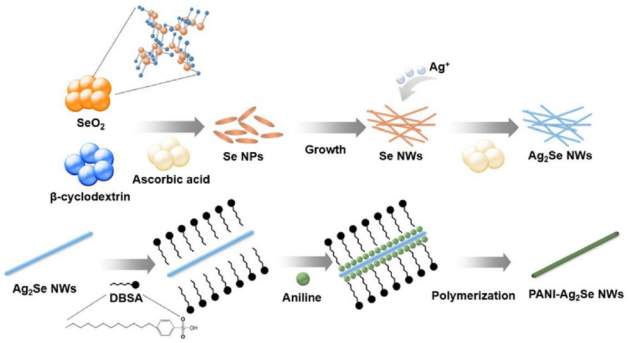

Fig. 11 Synthesis of polyaniline-Ag_2Se nanowires. [Reproduced from ref. 40, with permission from Elsevier, Copyright 2021.]

The resulting nanostructures, with sizes ranging from 80 to 100 nm, exhibited a core composed of Ag_2Te nanoparticles with a size of about 10 nm. When subjected to cold pressing, the Ag_2Te/polyaniline composite exhibited enhanced thermoelectric properties compared to pure Ag_2Te and polyaniline powders, with higher Seebeck coefficients and lower thermal conductivity. The core–shell nanocomposite had a special microstructure and interface between α-Ag_2Te and PANI, resulting in electrical conductivity (4.3 S m^{-1}) 5 order of magnitudes higher than that of PANI (6.53×10^{-5} S m^{-1}). The figure of merit (zT) of the nanocomposite was calculated to be 2.09×10^{-4}, which was slightly higher than that of α-Ag_2Te with a value of 2.00×10^{-4}.

Room temperature thermoelectric studies were reported for ternary hybrids comprised of PANI, MWCNTs, and binary inorganic selenide nanoparticles.[69] XRD confirmed their phase purity and FTIR indicated strong π–π interactions between PANI and MWCNTs. Furthermore, the electrical behaviour of the nanocomposites was examined, with Ag_2Se NPs/MWCNT/PANI showing p-type characteristics (zT of 0.012), while CuSe NPs/MWCNT/PANI showed excellent n-type thermoelectric behaviour. This study proposed future enhancements using conductive fillers and explored the potential impact of light on thermoelectric efficiency due to the photovoltaic effect of the materials. In this type of composite, the synthesis of Ag_2Te/PANI core/shell and ternary hybrid MWCNTs and binary selenides indicated the potential of nanocomposites for enhanced thermoelectric properties. Future research could focus on further optimizing synthesis techniques, exploring novel combinations of conductive fillers, and investigating the synergistic effects of light on thermoelectric performance, particularly regarding the photovoltaic capabilities of materials. This avenue of exploration holds promise for advancing thermoelectric technology and its applications in energy harvesting and conversion.

3.5. PANI/lead chalcogenides

Wang *et al.*[44] synthesized a PbTe/PANI nanocomposite by interfacial polymerization at room temperature. Core–shell PbTe-

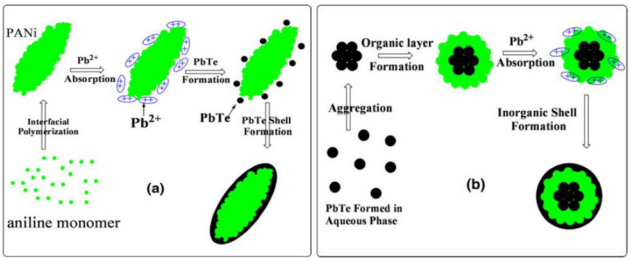

Fig. 12 Illustration of the growth mechanism for (a) PANI/PbTe core–shell structure and (b) PbTe/PANI/PbTe three-layer nanostructure. [Reproduced from ref. 44, with permission from Springer, Copyright 2011.]

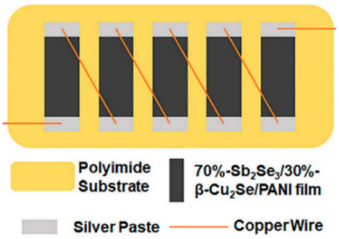

Fig. 13 TEG structure. [Reproduced from ref. 70, with permission from MDPI, Copyright 2021.]

PANI, PbTe nanoparticles and PbTe-PANI-PbTe three-layer spherical structure were obtained in the nanocomposite. The nanocomposite exhibited a higher Seebeck coefficient compared to its bulk counterpart due to its smaller particle size. The Seebeck coefficient decreased from 626 to 578 μV K^{-1} and the electrical conductivity increased from 1.9 to 2.2 S m^{-1} for a cold press composite pellet in the range of 293 to 373 K. The Seebeck coefficient value of the composite was the highest among the samples including PANI, PbTe and PbTe. However, the power factor of the composite was lower than that of the PbTe nanoparticles, where the extremely low thermal conductivity of the polymer makes the zT value of the composite higher.

The mechanism for the formation of the PANI/PbTe core–shell structure involved the PbTe aq. Phase, where PANI was present at the interface between the aq. phase and carbon tetrachloride (CCl_4) (water on oil type). It was discussed that the formation of PANI was faster than PbTe. Also, it was hypothesized that the initial PANI molecules penetrated the aqueous phase to absorb the Pb^{2+} ions through binding with their imino groups. This reaction generated a PbTe shell on the PANI core, finally yielding PbTe/PANI/PbTe nano-composite layers, as illustrated in Fig. 12. The process for the fabrication of PbTe/PANI nanocomposites has promising prospects for enhancing the thermoelectric properties. Future research can optimize the synthesis parameters to enhance the thermoelectric performance and explore diverse composite systems for broader applications.

3.6. PANI/copper chalcogenides

Upon incorporating copper selenide (Cu_2Se) in PANI, Sangamesha *et al.*[39] observed a red-shift in its UV-visible absorption band, suggesting the presence of an expanded coil-like polymer composite chain. It was also described that due to the ordered regularity and aligned nanostructure, shifting and sharpening of the quinoid, benzenoid and N–H stretching vibrations were observed in the FTIR spectra. The XRD spectra of the composite showed the semicrystalline nature of the composite with an increased PANI/Cu_2Se content compared with pure Cu_2Se. In continuation, to enhance the properties of copper selenide either alone or in combination with other metal selenides, Kim *et al.*[70] created two types of nanowire materials, Sb_2Se_3 and β-Cu_2Se. They synthesized Sb_2Se_3 through a hydrothermal reaction and produced β-Cu_2Se using a method involving the self-assembly induced by the evaporation of water. The electrical conductivities of these nanowires were enhanced by generating the conducting polymer PANI on their surfaces. Various combinations of Sb_2Se_3 and β-Cu_2Se were used and the film made of 70 : 30 Sb_2Se_3 : β-Cu_2Se with PANI showed the maximum power factor value of 181.61 μW m^{-1} K^{-2} at 473 K. Additionally, a thermoelectric generator (TEG) was assembled using five sections of this film, realizing the output power of 80.1 nW with a temperature difference (ΔT) of 30 K (Fig. 13). This study demonstrated the potential of flexible TEGs having a superior performance with the flexibility of polymers for future power generation in wearable or portable devices. The study conducted by Saray *et al.*[71] explored how combining PANI with Cu_xSe_y improves their photocatalytic performance and several factors were found to be responsible for the enhancement in activity. The most important one was the increased porosity of the Cu_xSe_y/PANI heterostructure, which enhanced the absorption of radiation, resulting in the greater generation of electron–hole pairs (EHPs). Also, the increased electrical conductivity facilitated the easy transfer of carriers during the redox process under light radiation. Additionally, the absorption of more photons was responsible for the better activities due to the presence of PANI. Overall, the type-II heterostructure nature of the composite enhanced its photocatalytic performance. The photocatalytic experiments targeting dye pollutant degradation under visible light revealed that Ag-PANI exhibited a stronger combined effect than pristine PANI composites in enhancing the photocatalytic function of the Cu_xSe_y nanostructure.[72] The improvement was ascribed to the enhanced textural properties, greater charge transfer, and unique surface plasmon resonance (SPR) properties of the Ag NPs, generating photogenerated electrons with higher potential.

3.7. PANI/cobalt chalcogenides

Sowbakkiyavathi *et al.*[73] synthesized CoSe nanoparticles (NPs) through a hydrothermal process, while polyaniline nanofibers (PANI NFs) were created *via* chemical polymerization. Subsequently, a CoSe/PANI NF composite formed through ultrasonication. This composite was studied for its role as a counter electrode (CE) in dye-sensitized solar cells (DSSC). The

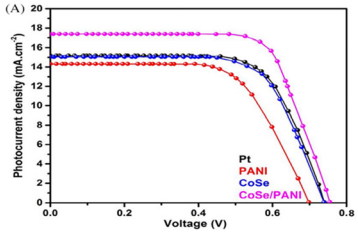

Fig. 14 DSSC photocurrent density *vs.* voltage (*J*–*V*) curve. [Reproduced from ref. 73, with permission from Wiley, Copyright 2021.]

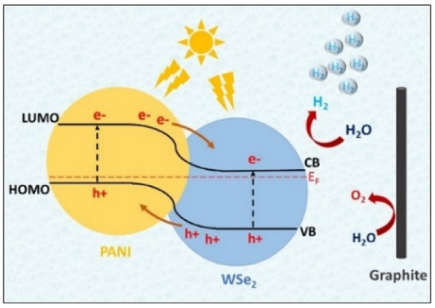

Fig. 15 Energy band structure with HER and OER in PANI/WSe_2 nanohybrid. [Reproduced from ref. 76, with permission from Elsevier, Copyright 2021.]

CoSe/PANI-based CE demonstrated excellent electrocatalytic action, exhibiting a small charge transfer resistance during the redox process. Therefore, a higher photocurrent density was achieved for the CoSe/PANI nanocomposite (Fig. 14). Notably, the DSSC incorporating the CoSe/PANI CE displayed a photoconversion efficiency of 9.14% under dark conditions. Gopalakrishnan *et al.*[74] successfully developed a novel binder-free 3D crumpled electrode, which was composed of $CoSe_2$ nanoparticles enveloped in polyaniline (PANI), using the co-electrodeposition method on Ni foam (PANI/$CoSe_2$/NF). The three-electrode cell setup showed remarkable results, with a specific capacitance of 1980 F g^{-1} and specific capacity of 792 C g^{-1} at 2 A g^{-1}. Also, this electrode exhibited an excellent performance in methanol oxidation, demonstrating a high current density of 139 mA cm^{-2}, low onset potential, and stable current response over 3000 s at 0.5 V. The PANI/$CoSe_2$/NF electrode shows future potential in energy storage, conversion, and catalysis, highlighting its broad impact across various domains. This electrode performed very well when oxidizing methanol, showing a consistent current response for 3000 s at 0.5 V, demonstrating its effectiveness.[75]

3.8. PANI/tungsten chalcogenides

The synthesis of stable and light-sensitive PANI/WSe_2 nanohybrids was reported by Kannichankandy *et al.*[76] as superior catalysts for the hydrogen evolution reaction (HER), showing a fast reaction with the low overpotential of −190 mV at −10 mA cm^{-2}. The infusion of electrons generated by light enhanced the production of hydrogen, facilitating the utilization of renewable energy sources. This improvement in electrocatalysis was due to the reduction in charge transfer resistance achieved through optimizing the composition of the nanocomposite. Overall, they achieved a notable photoresponsivity and the electrocatalytic hydrogen evolution reaction was sustained for about 42 h. The proposed mechanism of HER is depicted in Fig. 15. In a separate study, Cogal *et al.*[77] synthesized a Co-WSe_2/PANI electrocatalyst *via* the hydrothermal method, having a nanosheet structure. PANI played a crucial role in augmenting its electrochemical surface area and accelerating the reaction kinetics, and thus this material demonstrated a notable electrocatalytic performance in both the HER and oxygen evolution reaction (OER). This showed its potential as a promising bifunctional electrocatalyst for comprehensive water splitting. In another study, Sheela *et al.*[78] synthesized polyaniline nanofibers (PANI NFs) through a chemical oxidative polymerization procedure and tungsten di-selenide (WSe_2) NPs *via* a simple hydrothermal method. The electrochemical studies revealed that the WSe_2/PANI (1 : 1 wt%) CE displayed superior electrocatalytic characteristics for iodide/triiodide reduction compared to other compositions, pristine PANI, WSe_2, and standard platinum. Progressive research has unveiled the potential of PANI/WSe_2 nanohybrids and Co–WSe_2/PANI electrocatalysts in advancing renewable energy technologies. These materials demonstrate remarkable efficiency in hydrogen evolution and water splitting due to their optimized compositions, which enable rapid reaction kinetics and low overpotentials. Moreover, WSe_2/PANI composite nanofibers exhibit superior electrocatalytic behaviour, positioning them as promising alternatives to traditional Pt electrodes in dye-sensitized solar cells. These findings underscore the crucial role of efficient electrocatalysts in driving the transition towards sustainable energy solutions. Future endeavours should focus on refining compositions and scaling up production for widespread deployment in renewable energy systems.

3.9. PANI/molybdenum chalcogenides

Cogal *et al.*[79] successfully synthesized transition metal-doped $MoSe_2$/PANI by catalysing the polymerization of aniline in a hydrothermal environment. The structural and morphological analyses revealed the formation of flower-like nanoclusters with thin nanosheets, influenced by both transition metal doping (Co, Ni, Fe) and the integration of polyaniline (PANI).

The optimal conducting polymer composition was determined to be 100 mg of PANI and the co-doped $MoSe_2$/PANI catalyst demonstrated a better performance in both HER and OER in alkaline medium, surpassing that of its Ni- and Fe-doped counterparts. PANI played a crucial role in acting as a conducting template for holding the transition metal dichalcogenide (TMD) nanosheets and interacting with the transition metal, enhancing the catalytic activity. Notably, this catalyst exhibited high stability in both HER and OER, providing valuable insights for the construction of bifunctional electrocatalysts involving TMD materials, conducting polymers, and transition metal doping. Zhang *et al.*[80] reported the exceptional

specific capacitance of $MoSe_2$/PANI composite nanospheres formed by growing layered polyaniline (PANI) on mesoporous $MoSe_2$ nano-spheres, resulting from the synergic interplay between the rapid electron mobility of mesoporous $MoSe_2$ nanospheres and high pseudo-capacitance properties of PANI. The composite electrode exhibited a notable specific capacitance of 753.2 F g^{-1} at 1 A g^{-1}, with an impressive retention rate of 83% after 15 000 cycles. Furthermore, the $MoSe_2$/PANI// AC asymmetric supercapacitor (ASC) demonstrated a significant energy density of 20.1 W h kg^{-1} and power density of 650 W kg^{-1}, providing high-performance supercapacitor electrode materials for advanced application. Mittal *et al.*[81] conducted a study to examine how the dynamics of the charge carriers at the interface can be affected in nanocomposites of $MoSe_2$–PANI having different %weight ratios. Furthermore, these composites were applied in the photocatalytic degradation of Rhodamine-B dye and it was established that a 2 : 1 wt% ratio of $MoSe_2$ and PANI promoted the better transfer of electrons from PANI to $MoSe_2$. Thus, this reduced the recombination rate and improved the separation of charges. Consequently, there was a notable enhancement in the efficiency of photocatalytic degradation. Jin *et al.*[82] investigated the Goos-Hänchen (GH) shift in Kretschmann configuration when combined with 2D nanomaterials based on surface plasmon resonance (SPR). The theoretical analysis revealed that transition metal dichalcogenides (TMDCs), particularly monolayer $MoSe_2$, can enhance the GH shift and sensitivity. Varying layers of TMDCs in the Ag–TMDCs–PANI/chitosan hybrid structure resulted in both positive and negative GH shifts. The introduction of Cu^{2+} ions at a concentration of 30.8530 μM or 2.877 μM significantly altered the GH shift, and the Ag–WSe_2–PANI/chitosan structure demonstrated the optimal sensitivity of 2.426 × $10^6\lambda$/RIU. This suggested the potential application of the proposed structure in high-sensitivity sensors for chemical, biomedical, and optical sensing.

Zheng *et al.*[83] synthesized a core–shell $MoSe_2$–PANI composite through hydrothermal synthesis. The hollow microspheres demonstrated an enhanced active surface area, leading to increased charge storage. The contribution of surface capacitance increment could be estimated by the CV curves, which showed that the contribution was 49% at 5 mV s^{-1} and increased to 78% at 75 mV s^{-1} (Fig. 16). The $MoSe_2$–PANI electrode, having a mass ratio of 1 : 1, displayed the highest specific capacitance of 146.5 F g^{-1} under certain conditions. Additionally, the composite material demonstrated a notable energy density of 22.16 W h kg^{-1} and power density of 198 W kg^{-1}. Various factors contributed to the enhancement in its electrochemical performance.

Chen *et al.*[84] conducted a study, where they synthesized a new type of material for the fabrication of NH_3 gas sensors. They created composites by combining molybdenum ditelluride ($MoTe_2$) nanosheets with polyaniline (PANI) in the presence of HCl using the *in situ* chemical oxidation polymerization approach. The analysis of the composite structure revealed the presence of a porous mesh microstructure with PANI fibers attached to 2D $MoTe_2$ sheets. The $MoTe_2$/PANI

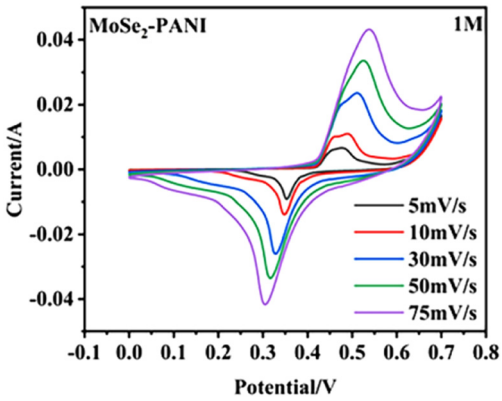

Fig. 16 CV curves at different scanning rates. [Reproduced from ref. 83, with permission from Springer, Copyright 2023.]

composites showed a much stronger response to NH_3 gas compared to pure PANI. In particular, the composites containing 8 wt% $MoTe_2$ showed a 4-fold increase in sensitivity of 1000 ppm NH_3 due to their increased surface area and formation of potential p–n heterojunctions (Fig. 17).

A MoSSe/polyaniline (PANI) composite was prepared by Khandare *et al.*[85] *via* hydrothermal and *in situ* oxidation polymerization methods, respectively. This composite exhibited a high specific capacitance of 340.6 F g^{-1} at 1 A g^{-1}, coupled with the low charge transfer resistance (R_{ct}) of 0.33 Ω. Due to the interaction between the active transition metal dichalcogenide (TMD) materials, thoughtful design involving redox chemistry, and robust storage capacity, an impressive 99.3% capacitance retention over extended cycles was achieved. These composites demonstrated enhanced catalytic activity, improved energy storage capabilities, and heightened sensitivity in sensors. Future investigations should focus on optimizing the synthesis methods, understanding the interfacial charge dynamics, exploring novel applications in catalysis and sensing, and ensuring the scalability and environ-

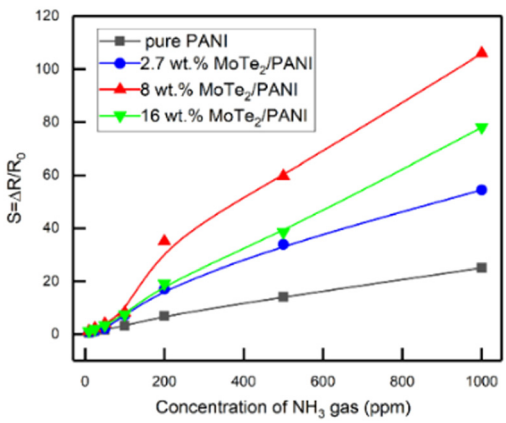

Fig. 17 Comparison of the sensing response of composites as a function of NH_3 gas concentration in the lab-environment. [Reproduced from ref. 84, with permission from MDPI, Copyright 2022.]

mental sustainability of these materials. Additionally, further research can delve into the integration of these composites in practical devices and systems for various technological advancements, presenting innovative solutions in energy storage, environmental monitoring, and beyond.

3.10. PANI/nickel chalcogenide & others

PANI composites have also been synthesized and studied using other chalcogenides, *e.g.*, NiSe carbon nanotubes coated with a polyaniline composite by Yang *et al.*,[86] who generated a controlled structure with enhanced electrochemical behaviour. The capacity of 529.3 mA h g^{-1} after 100 cycles at 0.1 A g^{-1} was realized when these researchers used NSC/PANI as an anode material. The ion diffusion behaviour analysis revealed its stable diffusion rate during cycling. The NSC/PANI//AC LICs exhibited a high capacity, retention and excellent rate performance, which achieved an energy density of 53.1 W h kg^{-1} at a power density of 1995.41 W kg^{-1}. Ju *et al.*[87] employed a combination of DBSA/PANI and coated tin selenosulphide, *i.e.*, $SnSe_{0.8}S_{0.2}$, to synthesise PANI-SnSeS nanosheets and utilized them in flexible thermoelectric generators. The optimization of the thermoelectric performance was dependent on the coating cycles. Another study introduced a solution-based method for incorporating PANI–SnSeS in a PVDF matrix in a 2 : 1 weight ratio, which exhibited remarkable durability with an enhanced thermoelectric outcome of about ~134 μW m^{-1} K^{-2} as the peak power factor at 400 K. Sowbakkiyavathi *et al.*[88] synthesized NiSe-embedded PANI nanofibers as counter electrodes in dye-sensitized solar cells (DSSCs). This composite material demonstrated superior electrocatalytic activity and achieved a higher photo-conversion efficiency compared to the pristine NiSe, PANI, and Pt counter electrodes. Besides, Yasoda *et al.*[89] produced an MnSSe/PANI heterostructure. They used a one-step solvothermal approach to replace S atoms with Se to generate MnSSe, on which the recrystallization of PANI nanorods was performed, increasing the conductivity and number of electroactive sites. This activity improved the crystallinity of the material, allowing charge carriers to move more easily in electrochemical reactions. This resulted in a 1.7 times higher specific capacitance for the MnSSe/PANI heterostructure than the individual components. Researchers also worked on metal composites containing PANI.[90–93] Oxygen reduction was accomplished by a 4 electron processes in the composite consisting of molybdenum-doped ruthenium selenide in a polyaniline matrix (PANI + MRS).[94] This property was realized because of the good conductivity and electrocatalytic property of the prepared material.

4. Applications

Various polyaniline composites with Se and Te and their metal chalcogenides have found a range of applications, *e.g.* in thermoelectric, optoelectronic, photocatalytic, sensors, bioimaging and EMI shielding (Scheme 2). Most of these applications and purposes were discussed in the respective section on the materials reviewed above. Nevertheless, a few additional examples are presented in this section to further show useful information in one place. Given that the same or similar materials were used for different applications, they are discussed as and when required.

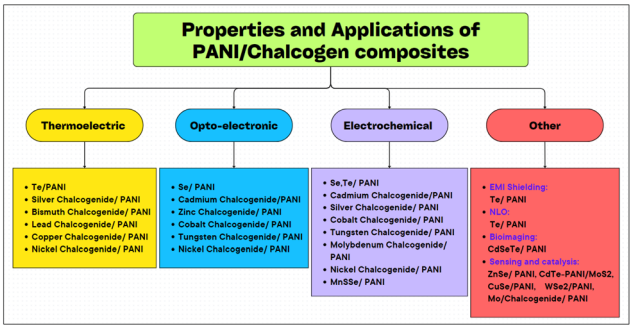

Scheme 2 Properties and applications of various chalcogen, chalcogenide/PANI composites.

In the case of thermoelectric applications, mostly polyaniline composites with silver, bismuth, lead, copper, nickel chalcogenides and tellurium have been studied. The power factor (PF) was reported to increase with the content of Te in these composite. The highest value was obtained for the Te-nanorod/PANI composite having 70 wt% Te, which was value of 101 μW m^{-1} K^{-2}.[28] Te nanorod/PANI with 60 wt% Te exhibited a PF of 50 μW m^{-1} K^{-2}.[32] However, ternary composites such as PANI/SWNT/Te nanorod (43 : 47 : 10 wt% ratio) showed an increase in PF up to 100 μW m^{-1} K^{-2}.[30] Alternatively, for PANI/MWCNT/Te nanorods with 50 wt% Te, the PF remained approx. 50 μW m^{-1} K^{-2}.[31] An electrodeposited film of Te on phenolic foam-coated PANI showed an increase in Seeback coefficient from 225 μV K^{-1} at 300 K to 342 μV K^{-1} at 473 K.[25] Te nanorod (70%)/PANI also showed an increase in PF to 25 μW m^{-1} K^{-2} with an increase in temperature to 150 K.[28]

Similarly, for electrochemical applications, composites of polyaniline with a wide variety of metals such as cadmium, silver, cobalt, tungsten, molybdenum, nickel, manganese chalcogenides and Se and Te have been studied.

The electrochemical and energy storage properties of many PANI/chalcogen composites have been reported. A graphene-encapsulated Se nanowire/PANI composite possessed a reversible charge–discharge capacity of 567 mA h g^{-1} at 0.2 C and 510.9 mA h g^{-1} at 2 C. The Se nanowire offers a short diffusion path for the Li-ion and the PANI shell increases the electrical conductivity by passivating the surface states, and also gives structural stability during charging–discharging. Besides, further encapsulation with graphene nanosheets improved the electrical conductivity by reducing the charge transfer resistance, increasing the speed of Li-ion diffusion.[22] In Te_xS_y@PANI nanorod materials for an Li–Te_xS_y battery, at a low charging rate (C-rate) of 0.1 A g^{-1} it worked as an Li–S battery having a high capacity of 1141 mA h g^{-1}, while at a high C-rate of 5 A g^{-1}, it showed Li–Te battery behaviour with excellent

cycling ability.[33] The specific capacitance was the highest for 10%-Te/PANI. A higher Te content reduced the ion migration and improved the stability.[34] Te/PANI (5–15%) showed ohmic behaviour in the dark and photo transport with variable resistance under illumination, with 10% Te/PANI exhibiting the lowest resistance and highest photocurrent. Te doping enhanced the conductivity and photocarrier generation, with 10% Te@PANI showing the superior performance.[34]

NiSe/CNT@PANI nanofibers were used in Li-ion capacitors (LIC) as an anode material. At a power density of 199.5 W kg^{-1}, the energy density was 91.7 W kg^{-1}, and at a higher power density of 1995.4 W kg^{-1}, the energy density was determined to be 53.1 W kg^{-1} in the fabricated LSC.[86]

NiSe/PANI nanofibers were used in a DSSC as the counter electrode (CE), achieving a photoconversion efficiency of 8.46%. It showed better electrocatalytic behaviour than pristine PANI and NiSe CE.[88] The applications of other composites were briefly discussed in the main sections (Scheme 2).

In the case of optoelectronic applications, the combination of polyaniline with chalcogenides of cadmium, zinc, cobalt, tungsten, and nickel as well as the individual elements Se and Te has been documented in the literature. Typically, CdSeTe QDs capped with PANI possessed enhanced fluorescence and blue shift in emission bands due to the surface trap passivation by PANI. Alternatively, they were shown to be a potentially good material for cell imaging, exhibiting a 1000 times increase in fluorescence at 450 nm when radiated at 360 nm. The zeta potential of the QDs increased from −29.9 mV to −53.1 mV upon capping with PANI.

The rare application of these composites in EMI was reported by us recently. In this unique study, were incorporated silver metal to enhance the electrical conductivity, which eventually yielded useful EMI shielding to the tune of about −10 dB. This composite also consisted of PVA to assist film fabrication. Te nanowires coated with PANI having a broom-shaped hierarchical structure were found to have non-linear optical (NLO) property.

5. General synthesis of composites of PANI with chalcogenides

The polymerization of aniline is accomplished by mainly two methods, chemical oxidative polymerization and electrochemical polymerization. Also, chalcogenides can be prepared using chemical methods such as solvothermal, hydrothermal, colloidal, sol–gel, electrochemical deposition and physical layer deposition (PLD).

In this case, the synthesis of composites of PANI with chalcogens and chalcogenides can be majorly categorized in four groups, as follows: (i) physical mixing, (ii) chemical mixing, (iii) electrochemical mixing, and (iv) catalytic *in situ* polymerization physical mixing, which can be accomplished by ultrasonic mixing, dip coating, incorporation of nanoparticles in the polymer matrix or spin coating. Some examples of the PANI/chalcogen composites formed in this way are PANI/Se,[20a]

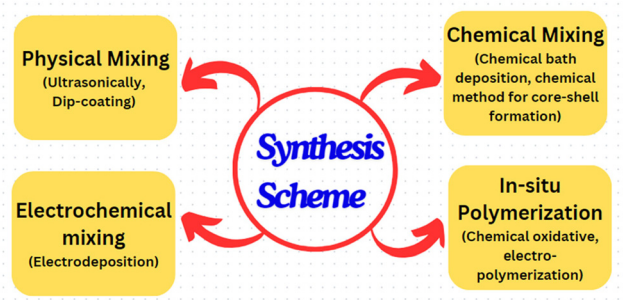

Scheme 3 Various methods for the synthesis of PANI/chalcogen nanocomposites.

Cu_2Se/PANI,[39] PANI/PEDOT:PSS/CdTe,[52] CSA:PANI/BST,[65] and CoSe/PANi.[73]

Chemical mixing is accomplished mainly by co-precipitation. The composite materials produced in this way are core–shell structures (ZnSe/PANI,[48] PANI/Bi_2Te_3,[42] PbTe/PANI/PbTe,[44] Ag_2Te/PANI,[68] and $MoSe_2$/PANI[83]), PANI/SWNT/Te,[30] PANI/Te,[32] ZnSe/PANI,[47a,49] and Co-WSe_2/PANI.[77] Electrochemical mixing is accomplished *via* the electrochemical deposition of PANI on the chalcogenide material, forming a heterostructure or intermixed composite. Some of these composites prepared in this way include Te/phenolic foam/PANI,[25] PANI/Se-Te,[29] CdX (X = S, Se, Te)/PANI,[35] ZnSe/PANI,[50] and CdTe/PANI.[54,58]

In the case of catalytic *in situ* polymerization, chalcogenides were first formed and dispersed in a solvent and the polymerization of aniline was performed *in situ* through chemical oxidative polymerization. Here, the polymerization happens due to catalytic action. A good example of this was reported by Yadav *et al.* for a Te/PANI nanocomposite.[36] Other composites prepared using this method include Se/PANI,[19,21] SeF/PANI,[24] Te/PANI,[27] CdSe/PANI,[5] C_{60}/CdSe/PANI,[37] PANI/Bi_2Se_3,[41] $MoTe_2$/PANI,[84] and MoSSe/PANI.[85]

Another version of *in situ* polymerization happens when aniline is electropolymerized in/on the chalcogenide. The composites and heterostructures formed this way include PANI/$CoSe_2$/Ni foam[74] and CZTSe/PANI (Scheme 3).[45]

6. Conclusions

Herein, we present a brief but informative review on Se, Te and their metal chalcogenides (two of the most versatile elements of the chalcogen group). These materials have been studied by numerous researchers in combination with polyaniline, which can be classified as PANI/chalcogenide nanocomposite materials, emphasizing their thermoelectric and electrochemical properties and their potential for energy conversion. Additionally, several researchers reported the chemical synthesis and characterization of tellurium-doped polyaniline, electrodeposition of tellurium films, and synthesis of PANI/Te nanocomposites with improved nonlinear optical properties. These findings offer promising avenues for the development of efficient energy utilization systems and multifunctional

materials, addressing the challenges posed by the global energy crisis. The preparation and characterization of PANI with selenium demonstrated significant improvements in electrical conductivity, thermal stability and field emission properties, making them useful materials in various electronic applications, such as vacuum micro-nano-electronic devices. From enhanced thermoelectric properties to improved fluorescence and biocompatibility, these materials hold promise for addressing various scientific and technological challenges. The synthesis methods discussed in various articles and covered in this review pave the way for further advancements in the field of nanocomposite materials. Recent research has extensively explored the multifaceted applications of polyaniline (PANI) composites, particularly when combined with various semiconductor nanoparticles such as CdSe, CdTe, and other metal chalcogenides. These studies provided valuable insights into the potential of PANI-based nanocomposites in electronic devices, optoelectronics, and thermoelectric applications. By incorporating semiconductor nanoparticles in PANI matrices through diverse synthesis methods, researchers have achieved significant improvements in conductivity, photovoltaic activities, and sensing capabilities. For instance, the successful fabrication of PANI/CdSe and PANI/CdTe nanocomposites resulted in enhanced electrical conductivity, improved photovoltaic activities, and potential applications in P–N junction diodes, gas sensors, and solar cells. Furthermore, the integration of metal chalcogenides such as $MoSe_2$ with PANI has shown promise in enhancing their thermoelectric performance, paving the way for potential applications in flexible thermoelectric devices and low-temperature thermoelectric systems. These advances highlight the versatility and promise of PANI-based composites in various technological fields. Looking ahead, future research efforts should focus on refining the synthesis techniques, optimizing the properties of nanocomposites, and exploring their integration in scalable devices. Additionally, addressing challenges related to stability, environmental impact, and performance optimization will be crucial for realizing the full potential of PANI-based composites in advancing technology and addressing societal needs.

Author contributions

Alok Yadav completed literature review, prepared draft of the review article, made some drawings and edited. Naeem Mohammad cross verified literature and the article along with correctness of the figures and references and obtained all copyright permissions also made some drawings, review and edited draft. Pawan Khanna reviewed the literature articles and edited the review draft, corrected, improved and finalized the manuscript along with students. Yogendra Kumar Mishra edited the received article and offered valuable suggestion in term of applications and synthesis methods. Elham Chamanehpour checked and corrected various sections and edited the manuscript in consultation with Yogendra Kumar Mishra. Data availability

This being a review article, various data presented in the manuscript are from the literature and they are presented in the manuscript with permission. The copyright permission obtained is available from the authors and will be provided on demand.

The original data if required may be demanded from the original author of the referenced articles.

Conflicts of interest

There are no conflicts to declare.

Acknowledgements

Authors thank Vice-chancellor DIAT for encouragement and support. NM thanks Govt. of India, India for DST INSPIRE fellowship for doctoral research (fellow no. IF200413). YKM acknowledges the fundings from the ESS Lighthouse on hard materials in 3D, SOLID (Danish Agency for Science and Higher Education, grant number 8144-00002B), Denmark, TORCH: (Interreg Deutschland-Denmark) and the European Union under grant number 04-3.2-23 2, and NANOCHEM (national infrastructure UFM 5229-00010B, NANOCHEM, Denmark).

References

1 H. Shirakawa, E. J. Louis, A. G. MacDiarmid, C. K. Chiang and A. J. Heeger, *J. Chem. Soc., Chem. Commun.*, 1977, 578–580.
2 A. J. Heeger, *J. Phys. Chem. B*, 2001, **105**, 8475–8491.
3 Z. Li, Y. Shen, Y. Li, F. Zheng, L. Liu, X. Liu and D. Zou, *High Perform. Polym.*, 2019, **31**, 178–185.
4 A. Eftekhari, L. Li and Y. Yang, *J. Power Sources*, 2017, **347**, 86–107.
5 R. Singh, A. K. Shrivastava and A. K. Bajpai, *Mater. Res. Express*, 2019, **6**, 1250a9.
6 K. G. B. Alves, E. F. De Melo, C. A. S. Andrade and C. P. De Melo, *J. Nanopart. Res.*, 2013, **15**, 1–11.
7 S. Koul, R. Chandra and S. K. Dhawan, *Polymer*, 2000, **41**, 9305–9310.
8 M. Khalid, A. M. B. Honorato and H. Varela, *Polyaniline: Synthesis Methods, Doping and Conduction Mechanism*, IntechOpen, 2018, pp. 1–17. DOI: **10.5772/intechopen.79089**.
9 F. X. Perrin and C. Oueiny, *React. Funct. Polym.*, 2017, **114**, 86–103.
10 A. Samadi, M. Xie, J. Li, H. Shon, C. Zheng and S. Zhao, *Chem. Eng. J.*, 2021, **418**, 129425.
11 Shumaila, G. B. V. S. Lakshmi, M. Alam, A. M. Siddiqui, M. Zulfequar and M. Husain, *Curr. Appl. Phys.*, 2011, **11**, 217–222.
12 A. Sezer, U. Gurudas, B. Collins, A. Mckinlay and D. M. Bubb, *Chem. Phys. Lett.*, 2009, **477**, 164–168.

13 R. Li, Z. Li, Q. Wu, D. Li, J. Shi, Y. Chen, S. Yu, T. Ding and C. Qiao, *J. Nanopart. Res.*, 2016, **18**, 1–11.
14 L. Zhang, T. Liu, R. Ren, J. Zhang, D. He, C. Zhao and H. Suo, *J. Hazard. Mater.*, 2020, **392**, 122342.
15 A. N. Gheymasi, Y. Rajabi and E. N. Zare, *Opt. Mater.*, 2020, **102**, 109835.
16 A. S. Roy, K. R. Anilkumar and M. V. N. A. Prasad, *J. Appl. Polym. Sci.*, 2012, **123**, 1928–1934.
17 V. V. A. Thampi, S. Thanka Rajan, K. Anupriya and B. Subramanian, *J. Nanopart. Res.*, 2015, **17**, 1–12.
18 R. B. Gapusan and M. D. L. Balela, *Polym. Bull.*, 2022, **79**, 3891–3910.
19 E. Bormashenko, R. Pogreb, S. Sutovski, A. Shulzinger, A. Sheshnev and A. Gladkikh, *Synth. Met.*, 2003, **139**, 321–325.
20 (*a*) Shumaila, S. Parveen, M. Alam, A. M. Siddiqui and M. Husain, *J. Nanosci. Nanotechnol.*, 2015, **15**, 2835–2839; (*b*) R. H. Fowler and L. Nordheim, *Proc. R. Soc. of Lond. A*, 1928, **119**, 173–181.
21 E. Ozkazanc, S. Zor and H. Ozkazanc, *J. Macromol. Sci., Part B: Phys.*, 2012, **51**, 2122–2132.
22 J. Zhang, Y. Xu, L. Fan, Y. Zhu, J. Liang and Y. Qian, *Nano Energy*, 2015, **13**, 592–600.
23 W. Ye, K. Wang, W. Yin, W. Chai, Y. Rui and B. Tang, *Dalton Trans.*, 2019, **48**, 10191–10198.
24 Z. K. Heiba, M. B. Mohamed and N. G. Imam, *J. Supercond. Novel Magn.*, 2019, **32**, 2981–2986.
25 C. H. Jiang, W. Wei, Z. M. Yang, C. Tian and J. S. Zhang, *J. Porous Mater.*, 2012, **19**, 819–823.
26 S. Kazim, V. Ali, M. Zulfequar, M. M. Haq and M. Husain, *Curr. Appl. Phys.*, 2007, **7**, 68–75.
27 J. Wang, X. Zhang, R. Ke, S. Zhang, C. Mao, H. Niu, J. Song, S. Li and Y. Tian, *Semicond. Sci. Technol.*, 2016, **31**, 1–10.
28 Y. Wang, S. M. Zhang and Y. Deng, *J. Mater. Chem. A*, 2016, **4**, 3554–3559.
29 T. Xue, X. Wang, S. K. Kwak and J. M. Lee, *Ind. Eng. Chem. Res.*, 2013, **52**, 5072–5078.
30 L. Wang, Q. Yao, W. Shi, S. Qu and L. Chen, *Mater. Chem. Front.*, 2017, **1**, 741–748.
31 Y. Wang, C. Yu, M. Sheng, S. Song and Y. Deng, *Adv. Mater. Interfaces*, 2018, **5**, 3–8.
32 Y. Wang, C. Yu, G. Liu, M. Sheng and Y. Deng, *Mater. Lett.*, 2018, **229**, 293–296.
33 J. Li, Y. Yuan, H. Jin, H. Lu, A. Liu, D. Yin, J. Wang, J. Lu and S. Wang, *Storage Mater.*, 2019, **16**, 31–36.
34 P. Rani, Y. Jewariya, K. K. Haldar, R. Biswas and P. S. Alegaonkar, *J. Mater. Sci.: Mater. Electron.*, 2023, **34**, 8.
35 S. S. Joshi and C. D. Lokhande, *J. Mater. Sci.*, 2007, **42**, 1304–1308.
36 A. K. Yadav, N. Mohammad and P. K. Khanna, *Mater. Adv.*, 2023, **4**, 4409–4416.
37 E. Rusen, A. Diacon, A. Mocanu and L. C. Nistor, *Sci. Rep.*, 2016, 32237, DOI: **10.1038/srep32237**.
38 G. R. Bhand, M. G. Lakhe, A. B. Rohom, P. U. Londhe, S. K. Kulkarni and N. B. Chaure, *J. Mater. Sci.: Mater. Electron.*, 2017, **28**, 12555–12563.
39 M. A. Sangamesha, K. Pushpalatha and G. L. Shekar, *Indian J. Adv. Chem. Sci.*, 2014, **2**, 223–227.
40 D. Park, M. Kim and J. Kim, *J. Alloys Compd.*, 2021, **884**, 161098.
41 M. Mitra, C. Kulsi, K. Kargupta, S. Ganguly and D. Banerjee, *J. Appl. Polym. Sci.*, 2018, **135**, 46887.
42 K. Chatterjee, M. Mitra, K. Kargupta, S. Ganguly and D. Banerjee, *Nanotechnology*, 2013, **24**, 215703.
43 V. B. Reddy, P. L. Garrity and K. L. Stokes, *RS Online Proc. Libr.*, 2003, **793**, 354–358.
44 Y. Y. Wang, K. F. Cai, J. L. Yin, B. J. An, Y. Du and X. Yao, *J. Nanopart. Res.*, 2011, **13**, 533–539.
45 K. Urazov, M. Dergacheva, A. Tameev, O. Gribkova and K. Mit, *J. Solid State Chem.*, 2021, **25**, 237–245.
46 E. Bormashenko, R. Pogreb, S. Sutovski, A. Shulzinger, A. Sheshnev, G. Izakson and A. Katzir, *Synth. Met.*, 2004, **140**, 49–52.
47 (*a*) D. Kaushik, M. Sharma, R. Raj Singh, D. K. Gupta and R. K. Pandey, *Mater. Lett.*, 2006, **60**, 2994–2997; (*b*) N. Kumbhojkar, S. Mahamuni, V. Leppert and S. H. Risbud, *Nanostruct. Mater.*, 1998, **10**(2), 117.
48 A. Shirmardi, M. A. M. Teridi, H. R. Azimi, W. J. Basirun, F. Jamali-Sheini and R. Yousefi, *Appl. Surf. Sci.*, 2018, **462**, 730–738.
49 F. S. Shokr and S. A. Al-Gahtany, *Polym. Compos.*, 2018, **39**, 1724–1730.
50 A. N. Jijana, *Appl. Biochem. Biotechnol.*, 2023, **195**, 3425–3455.
51 D. N. Ahilfi, A. S. Alkabbi, K. A. Mohammed and K. M. Ziadan, *IOP Conf. Ser.: Mater. Sci. Eng.*, 2020, **928**, 072069.
52 M. Patullo and M. A. Sahiner, PANI and PEDOT:PSS Dip-Coating on CdS/CdTe Solar Cells, 2018. [Online]. Available: **https://scholarship.shu.edu/locus/vol1/iss1/9**.
53 L. Mekhiche, N. Maouche, B. Nessark, L. Toukal and H. Ayadi, *J. Adhes. Sci. Technol.*, 2021, **35**, 2602–2624.
54 N. P. Gaponik, D. V. Talapina and A. L. Rogachb, *Phys. Chem. Chem. Phys.*, 1999, **1**, 1787–1789.
55 J. Xue, X. Chen, S. Liu, F. Zheng, L. He, L. Li and J.-J. Zhu, *ACS Appl. Mater. Interfaces*, 2015, **7**, 19126–19133.
56 S. S. Joshi, C. D. Lokhande and S. H. Han, *Sens. Actuators, B*, 2007, **123**, 240–245.
57 S. S. Joshi, T. P. Gujar, V. R. Shinde and C. D. Lokhande, *Sens. Actuators, B*, 2008, **132**, 349–355.
58 D. Verma and V. Dutta, *J. Appl. Phys.*, 2009, **105**, 034904.
59 N. A. Abdul-Manaf, O. K. Echendu, F. Fauzi, L. Bowen and I. M. Dharmadasa, *J. Electron. Mater.*, 2014, **43**, 4003–4010.
60 P. H. F. M. Junior, A. F. L. Almeidaa, R. L. Moreiraa, E. S. Teixeraa, V. F. Nunesa, D. C. Pinhoa and F. N. A. Freire, *Mater. Res.*, 2021, **24**, 1–9.
61 D. Xu, M. Yang, Y. Liu, R. Zhu, X. Lv, C. Zhang and B. Liu, *J. Alloys Compd.*, 2020, **822**, 153685.
62 D. Liu, Q. Gong, X. Xu, S. Meng, Y. Li and T. You, *J. Electroanal. Chem.*, 2023, **930**, 117143.
63 S. Subramanian and D. P. Padiyan, *Mater. Chem. Phys.*, 2008, **107**, 392–398.

64 K. Chatterjee, A. Suresh, S. Ganguly, K. Kargupta and D. Banerjee, *Mater. Charact.*, 2009, **60**, 1597–1601.
65 C. Guo, F. Chu, P. Chen, J. Zhu, H. Wang, L. Wang, Y. Fan and W. Jiang, *J. Mater. Sci.*, 2018, **53**, 6752–6762.
66 A. V. Zhmurova, G. F. Prozorova and M. V. Zvereva, *Powders*, 2023, **2**, 540–561.
67 G. S. Hegde, A. N. Prabhu, S. Putran, M. Y. Bhat and P. D. Babu, *J. Mater. Sci.: Mater. Electron.*, 2023, **34**, 1896.
68 Y. Y. Wang, K. F. Cai, J. L. Yin, Y. Du and X. Yao, *Mater. Chem. Phys.*, 2012, **133**, 808–812.
69 A. S. Kshirsagar, C. Hiragond, A. Dey, P. V. More and P. K. Khanna, *ACS Appl. Energy Mater.*, 2019, **2**, 2680–2691.
70 M. Kim, D. Park and J. Kim, *Polymers*, 2021, **13**, 1518.
71 A. M. Saray, H. Azimi, A. Shirmardi, M. Nouri and R. Yousefi, *J. Alloys Compd.*, 2023, **951**, 169827.
72 A. M. Saray, H. Azimi, A. Shirmardi, M. Nouri and R. Yousefi, *Surf. Interfaces*, 2023, **42**, 103416.
73 E. S. Sowbakkiyavathi, V. Murugadoss, R. Sittaramane, R. Dhanusuraman and S. Angaiah, *Polym. Adv. Technol.*, 2021, **32**, 3137–3149.
74 A. Gopalakrishnan and S. Badhulika, *Mater. Chem. Phys.*, 2021, **273**, 125118.
75 A. Gopalakrishnan and S. Badhulika, *J. Energy Storage*, 2021, **41**, 102853.
76 D. Kannichankandy, P. M. Pataniya, C. K. Sumesh, G. K. Solanki and V. M. Pathak, *J. Alloys Compd.*, 2021, **876**, 160179.
77 S. Cogal, G. Celik Cogal, M. Mičušík, M. Kotlár and M. Omastová, *Int. J. Hydrogen Energy*, 2024, **49**, 689–700.
78 S. E. Sheela, V. Murugadoss, R. Sittaramane and S. Angaiah, *Sol. Energy*, 2020, **209**, 538–546.
79 S. Cogal, G. C. Cogal, M. Mičušík, A. Michalcova, M. Šlouf and M. Omastová, *J. Electroanal. Chem.*, 2023, **946**, 117728.
80 H. Zhang, G. He, D. Zheng, H. H. Fu, Y. Li, Y. Mi, M. Wu and H. Yuan, *Nanotechnology*, 2023, **41**, 28–34.
81 H. Mittal and M. Khanuja, *Mater. Today: Proc.*, 2020, **28**, 314–316.
82 M. Jin, J. Liu, W. Xu, D. Deng and L. Han, *Plasmonics*, 2023, **18**, 1129–1141.
83 D. Zheng, G. He, Y. Mi, H. H. Fu, Y. Li, H. Zhang, M. Wu and H. Yuan, *J. Mater. Sci.: Mater. Electron.*, 2023, **37**, 1734.
84 X. Chen, X. Chen, X. Ding and X. Yu, *Chemosensors*, 2022, **10**, 1–15.
85 L. N. Khandare, D. J. Late and N. B. Chaure, *Surf. Interfaces*, 2023, **43**, 103533.
86 F. Yang, Z. Zhang, H. Li, W. Dong, M. Li, M. Zhao, M. Xue and Q. Zhang, *Mater. Today Commun.*, 2024, **38**, 107816.
87 H. Ju, D. Park and J. Kim, *ACS Appl. Mater. Interfaces*, 2018, **10**, 11920–11925.
88 E. S. Sowbakkiyavathi, V. Murugadoss, S. P. Rajendra, M. S. AlSalhi, P. Dhandapani and S. Angaiah, *J. Mol. Struct.*, 2024, **1305**, 137735.
89 K. Yamini Yasoda, M. Afshan, S. Charis Caroline, E. M. Harini, K. Ghosh and S. K. Batabyal, *Electrochim. Acta*, 2024, **480**, 143879.
90 A. Güngor, S. G. Çolak, M. O. Alaş Çolak, R. Genç and E. Erdem, *Electrochim. Acta*, 2024, **480**, 143924.
91 K. Y. Yasoda, S. Kumar, M. S. Kumar, K. Ghosh and S. K. Batabyal, *Mater. Today Chem.*, 2021, **19**, 100394.
92 M. Khosya, D. Kumar, M. Faraz and N. Khare, *Int. J. Hydrogen Energy*, 2023, **48**, 2518–2531.
93 S. Suresh, H. C. Prakash, M. Sathish Kumar and S. K. Batabyal, *J. Sci.: Adv. Mater. Devices*, 2023, **8**, 100639.
94 N. Alonso-Vante, S. Cattarin and M. Musiani, *J. Electroanal. Chem.*, 2000, **481**, 200–207.